A Home-Made Passive Direct Methanol Fuel Cell

A Major Qualifying Report

Submitted to the faculty of
Chemical Engineering Department
Worcester Polytechnic Institute
Worcester, MA 01609

April 30th, 2009

By:

Neal Rosenthal

Approved by:

Prof. Ravindra Datta

Table of Contents

Table of Figures

List of Tables

Abstract

"Active" Direct Methanol Fuel Cells (DMFC) must rely on equipment to run whereas passive DMFCs can run in ambient conditions without any equipment, allowing for potential use in portable devices. In this report, a passive DMFC was designed and constructed with the potential of being equivalent to a battery then compared to an active DMFC and a battery. Passive DMFCs, while not as good performance-wise as active DMFCs, perform notably better than a battery as an energy source.

Introduction

Fuel cells are a unique energy source to the industry and population. Like a combustion engine, as long as a fuel supply is provided, fuel cells can provide an indefinite amount of energy. And like batteries, fuel cells rely on electrochemistry to produce energy, contain no external moving parts, and work silently. In addition, fuel cells produce nearly no particulate emissions and harmful products that may affect the environment (O'Hayre et al., 2006).

While fuel cells are advantageous in several ways, there are several issues that must be overcome. Fuel cells are economically unattractive due to their high costs. In addition, while methanol fuel has a theoretical power density of 10 times more than lithium-ion batteries (Yang et al., 2006), fuel cells cannot produce nearly as much volumetric power density as combustion engines. Another issue in fuel cells is that the fuel may require reforming into hydrogen, which drops the performance of the fuel cell even further. Other concerns include the operational temperature of the fuel cell and any environmental hazards the fuel cell may cause (O'Hayre et al., 2006).

Several types of fuel cells are currently being developed in the industry, including Phosphoric Acid Fuel Cells (PAFC), Polymer Electrolyte Membrane Fuel Cells (PEMFC), Alkaline Fuel Cells (AFC), Molten Carbonate Fuel Cells (MCFC), Solid-Oxide Fuel Cells (MOFC), and, the focus of this report, Direct Methanol Fuel Cells (DMFC).

DMFCs have several advantages over the other types of fuel cells. One advantage is that they can work at temperatures below 100ºC, a suitable working temperature, as opposed to PAFCs operating temperature of 200ºC or MCFCs operating temperature of 650ºC (O'Hayre et al., 2006). Another advantage is the use of methanol in the fuel cell; because methanol is a liquid at room temperature, it is easy to store and refill as a fuel source as opposed to hydrogen. In addition, methanol has a high energy density compared to hydrogen, which can be a promising asset as a power source for portable devices and micropower sources (Lu et al., 2006).

Describing the DMFC

DMFCs consists of several parts: an anode and cathode bipolar plates, two gaskets, an anode and cathode gas diffusion layer (GDL), an anode and cathode catalyst layer, and a Proton Exchange Membrane (PEM) (Figure 1). The bipolar plates on the outside of the cell, usually constructed from metal or graphite, allow methanol to flow on the anode side and oxygen on the cathode side through a unique flow pattern. The methanol flowing through the anode bipolar plate makes contact with the anode GDL and disperses to the anode catalyst layer where it reacts, producing carbon dioxide, protons, and electrons, while the oxygen being supplied to the cathode GDL and thence to the cathode catalyst layer, reacts with protons and electrons arriving from the anode to form water. The gaskets, typically made from Teflon, must be about the same width of the catalyst layer and GDL combined in order to prevent the methanol and oxygen from leaking out of the fuel cell. The PEM, the catalyst layer, and the GDLs are prepared together, forming a Membrane Electrode Assembly (MEA).

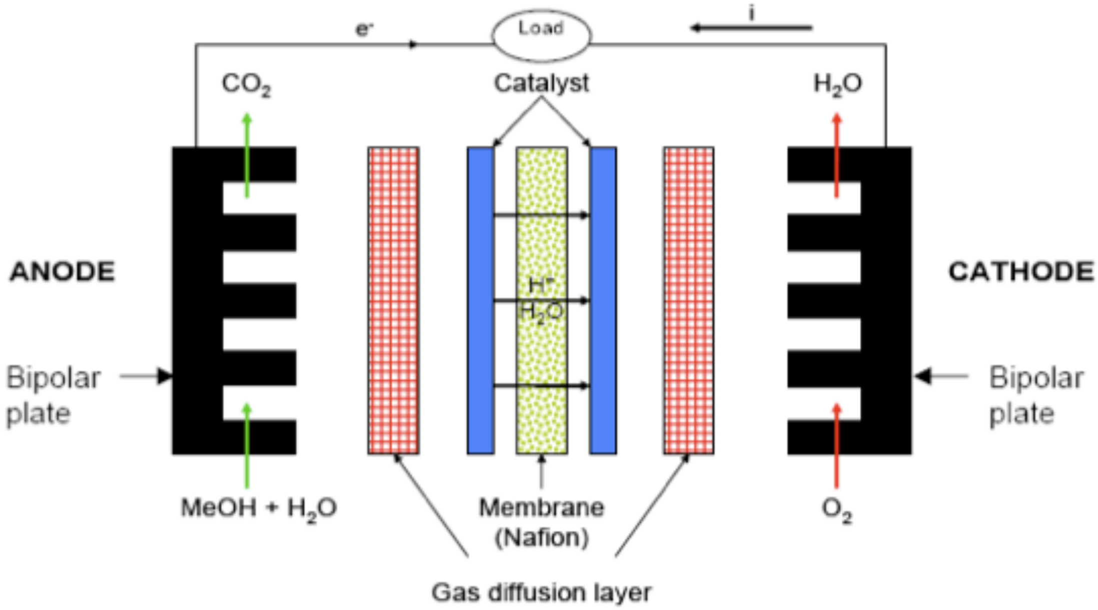

Figure 1: Diagram of a DMFC (Hackquard, 2008)

The most common material used in a GDL can be either carbon fiber paper or woven carbon cloth. While the carbon fiber paper provides a high level of electron conductivity, the carbon cloth is more advantageous due to its improved water management, improving performance. The GDL is responsible for distributing the methanol/oxygen to the catalyst. Once the supplied fuel supply reacts with the catalyst, the GDL then conducts the electrons created from the reactions (Hoogers, 2003). The electrons in the GDL are redirected into the bipolar plates and through an external circuit; if an external load box is used, the current provided by the electrons can be measured.

The composition of the catalyst layers for the anode and cathode have slightly different compositions based on the task they were meant to perform. The preferred anode catalyst loading consists of platinum and ruthenium, carbon supported, while the preferred cathode catalyst loading only contains platinum, carbon supported. The support on carbon allows for more efficient particle dispersion (Arbizzani et al., 2007). In the first step, the platinum allows for the oxidation of methanol into carbon monoxide, as shown in equation (1).

$$CH_3OH \rightarrow CO + 4H^+ + 4e^- \qquad (1)$$

Unfortunately, carbon monoxide poisons the anode catalyst and prevents the methanol to react further. To resolve this issue, the ruthenium in the anode oxidizes the water into a hydroxide radical at an appropriate over potential in the next step, which subsequently reacts with the carbon monoxide to produce carbon dioxide as shown in equations (2) and (3).

$$H_2O \rightarrow OH\bullet + H^+ + e^- \qquad (2)$$

$$CO + OH\bullet \rightarrow CO_2 + H^+ + e^- \qquad (3)$$

The final result is an overall oxidation half-reaction at the anode catalyst layer, shown in equation (4).

$$CH_3OH + H_2O \rightarrow CO_2 + 6H^+ + 6e^- \qquad (4)$$

As mentioned before, the electrons are conducted by the anode GDL and transported to the cathode GDL via an external circuit. Meanwhile, the protons are conducted through the PEM from the anode to the cathode.

The PEM used in a standard MEA is a preflourosulfonated ionomer membrane, commonly referred to as a Nafion membrane, a registered trademark of DuPont (Chen et al., 2007). The Nafion membrane is a good proton conductor, allowing dissociated protons from the reacting methanol to pass through the membrane. The protons are carried over to the cathode catalyst loading, where the reduction half-reaction occurs.

At the cathode side of the DMFC, the electrons that were produced at the anode arrive at the cathode catalyst via the cathode GDL. Combining with the dissociated protons carried over through the Nafion membrane and a supply of oxygen provided by the cathode bipolar plate, the oxygen goes through a reduction half-reaction and is converted into water, as shown in reaction (5).

$$3/2O_2 + 6H^+ + 6e^- \rightarrow 3H_2O \qquad (5)$$

Combining the two half reactions, the overall fuel cell reaction consumes methanol and oxygen and produces carbon dioxide and water, as shown in equation (6).

$$CH_3OH + 3/2O_2 \rightarrow CO_2 + 2H_2O \qquad (6)$$

Losses in Performance

Figure 2 represents a general performance curve of a DMFC. Its performance is measured in cell voltage versus the current density. Unfortunately, the performance curve is plagued by many types of losses in several areas. The optimal open circuit potential (OCP), the case when a fuel cell is operating with no current density, should be about 1.2 V according to thermodynamics. However, an average DMFC OCP is usually 0.65 V (Schultz et al., 2001). This is beause of methanol crossover from the anode to the cathode, causing both half cell reactions to occur at the cathode, thus causing a cathode overpolarization, even at zero entered current. Region 1 in Figure 2 represents the activation polarization represented by Butler-Voluner equation. Losses in this region occur from the activation of the anode and cathode electrodes, which slow down the reaction rate. Region 2 corresponds to the Ohmic polarization. Ohm's Law, as shown in equation (7), represents this drop in performance.

$$V = IR \qquad (7)$$

Where V is the voltage, I is the current, and R is the resistance and slope of the performance curve only in region 2. This drop corresponds to the proton conductivity of the PEM at higher current densities. Region 3 represents the concentration polarization. The drop in performance in this region occurs due to the mass transfer limitations, such as the slow reactant feed to the reactant sites, slow proton transport, or slow carbon dioxide and water byproduct removal.

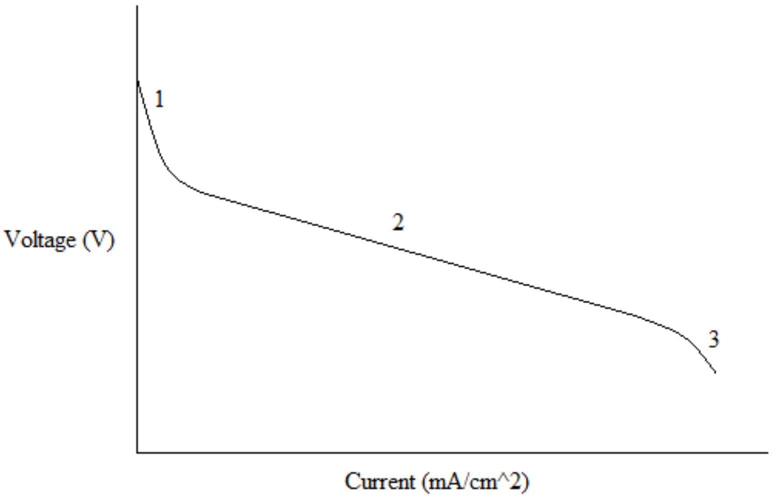

Figure 2: Polarization of a DMFC

Passive Direct Methanol Fuel Cells

Standard DMFC systems are generally overly complex, have parasitic power losses due to the auxiliary equipment's detrimental effects on the net power density (Liu et al., 2005), require large volume, and have a high cost. Due to these issues, an alternative form of DMFC operation is being developed: a passive direct methanol fuel cell, or a DMFC that relies on breathing ambient air rather than oxygen flow and no pumping of methanol fuel. The reacting reduction in size and increased simplicity have given passive DMFCs more attention over standard DMFCs, as the reduced size would allow functionality in portable devices such as cell phones and PDAs (Shimizu, 2004).

Figure 3 shows a diagram of a passive DMFC. The passive DMFC, like a conventional DMFC, contains an MEA, gaskets, and two current collectors. The main difference is the storage of methanol and supply of oxygen. On the anode side, the methanol is held in a small reservoir as opposed to being continuously pumped. On the cathode side, an opening has been provided for air to flow in naturally versus oxygen being fed to the cathode.

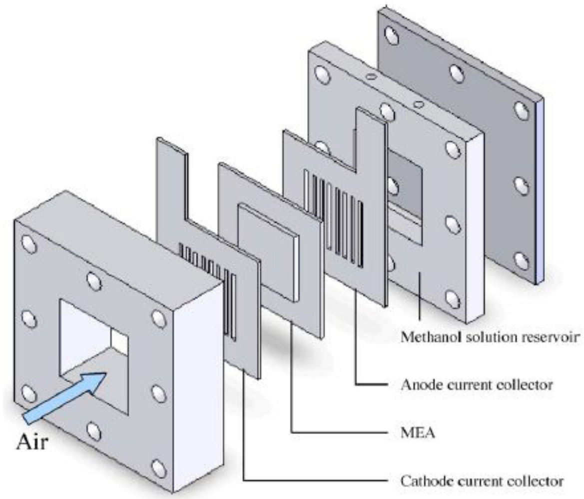

Figure 3: Passive DMFC Setup (Liu et al., 2005)

Goals of this Project

1. The properties of the fuel source determine how well a DMFC performs. A recent study in our laboratory determined the performance of a DMFC with varying liquid methanol concentrations, membrane thickness, and temperature (Field, 2008). Continuing from this research, a vapor feed of methanol was also tested. The vapor feed was tested between two different methanol molarities (3M, 5M) as well as two different Nafion membrane thicknesses (1035, 115).

2. Using the tools available, a passive DMFC was constructed. The contents of the passive home-made fuel cell consisted of the following: the fuel source (liquid methanol, methanol gel, or vapor fuel from a beaker containing methanol) contained within it, several gaskets, two current collectors, and a home-made MEA. The fuel source and MEA used were based on Field’s results as well as the results derived from the vapor feed testing.

3. Once the home-made fuel cell was functional, all four sides of the fuel cell were fitted with MEAs and tested. The MEAs were connected in series through the current collectors, providing a cumulative voltage but same current for the four MEAs. In addition, a device was powered by the home-made fuel cell.

Literature Review

The concept of making a home-made passive fuel cell is a unique idea; there are not that many articles on this type of technology. Faghri and Guo's (2008) built passive fuel cell with several features: a planar fuel cell stack, a feed consisting of pure methanol, reliance on ambient air rather than a feed of oxygen, no pumps or external power sources, a passive water recirculation system, the ability to operate in any position, and cost efficacy. Figure 4 shows the mechanism that allowed the passive DMFC to function in any position rather than relying on gravity to carry the methanol vapor to the anode. Methanol is transferred from the hydrophobic medium to the water in the hydrophilic medium via a cotton wick. This concept was expanded to apply to the larger scale passive DMFC. The wick can also control the concentration of methanol entering the anode.

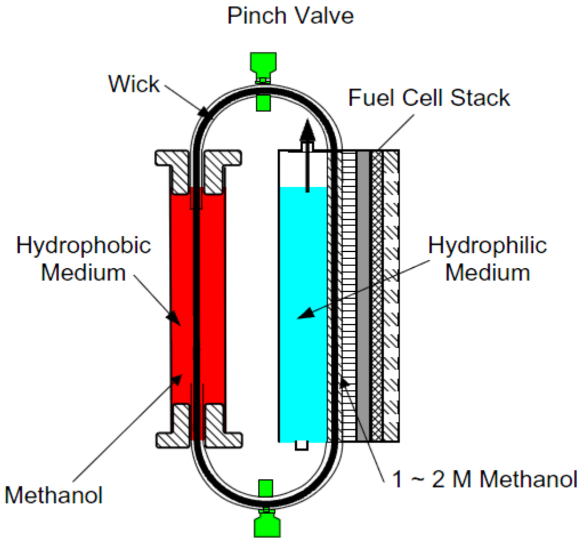

Figure 4: Orientation-Dependent Mechanism (Faghri et al., 2008)

The end result of the passive fuel cell design is shown in Figure 5. No external equipment was required to run this fuel cell, an exceptional feature in the development of DMFCs. The fuel stack on the front of the fuel cell contains four cells stacked in series; the voltages will stack up to a cumulative sum while the currents will be equal among the four cells.

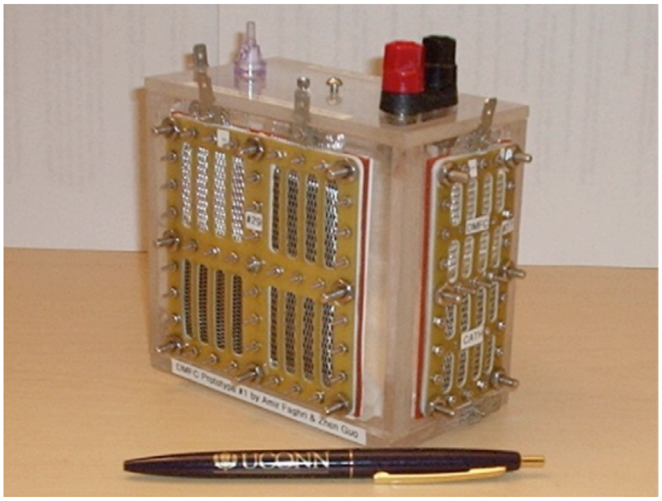

Figure 5: Passive DMFC Prototype (Fagri et al., 2008)

Figure 6 shows the testing of the constructed passive DMFC at 1M, 2M, 3M, and 5M. Because the cell stacks are connected in series, the voltage is about 4 times larger than a standard DMFC polarization curve at OCP. However, this increase does not affect the current density or power density. In the low current density region, 1M performs the best while 5M performs the worst. In the high current density region, 2M outperforms all of the other concentrations while 1M does not perform very well.

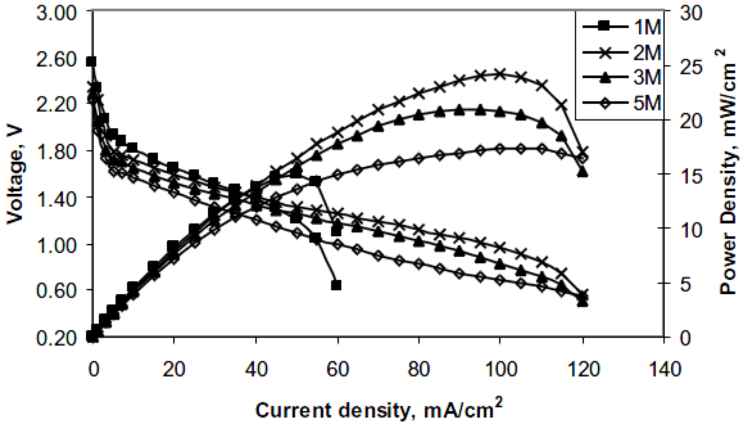

Figure 6: Polarization Curves of the Constructed Passive DMFC

Kim et al. (2003, 2005) has explored the concept of a monopolar stack (Figure 7) operating in passive conditions. The monopolar stack consists of six MEA strips, or cells, with an active area of 4.5 cm^2. With 4M methanol, the monopolar stack provided an output of 1000 mW, or 37 mW/cm^2. The stack was later tested in several areas with respect to time. The monopolar stack OCP was maintained at its highest with 1M methanol, but provided the lowest stack temperature. Using 4M methanol, while it provided the worst stable OCP, it supplied the highest stack temperature. Because temperature is directly correlated to the performance of the fuel cell, the current density of the monopolar stack using 4M methanol will be the highest, despite its low OCP. In addition, the outermost cells suffered the most heat loss due to their position; the inner four cells had a higher cell temperature than the outer cells.

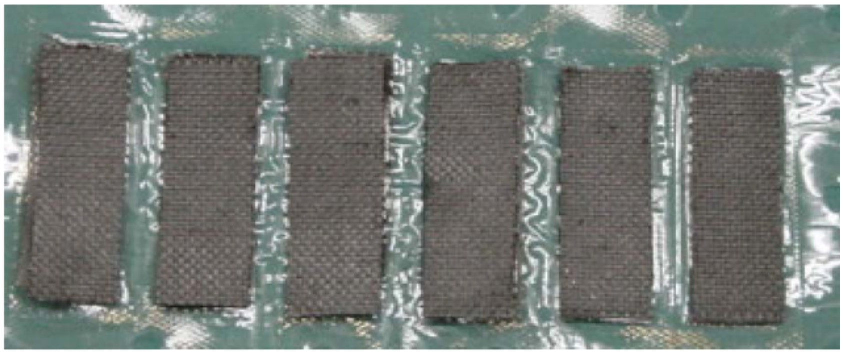

Figure 7: A Monopolar Stack With Six Single Cells (Kim et al., 2003)

Baglio et al. (2008) tested two different current collector cutouts using a monopolar stack with three single cells. The left of Figure 8 is a cell stack of three cells with individual holes cut into the current collectors while the right of Figure 8 is another cell stack with a hole cut out to the size of the GDL. Between the two cell stacks, both had advantages and disadvantages. The left fuel stack provided a higher stack voltage at OCP due to a lower methanol crossover, while the right fuel stack had a higher voltage at high current densities, demonstrating better mass transport capabilities. In addition, the right fuel stack discharge time was more than three times longer than the left fuel stack due to the improved mass transport characteristics and easier carbon dioxide removal.

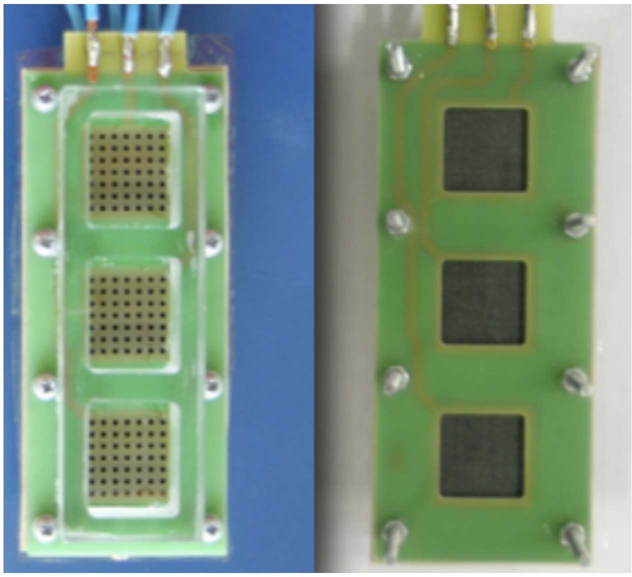

Figure 8: Two Monopolar Stacks With Varying Current Collectors

Active Versus Passive

The most notable difference between an active DMFC and passive DMFC is the amount of equipment used; because passive DMFCs run in completely ambient conditions, it has a simple and compact setup that requires no equipment. The setback to this convenience is the impact to its performance. Eccarius et al. (2008) performed a series of experiments, varying the anode and cathode parameters between an active setup and passive setup.

Table 1 and Figure 9 represent polarization curve comparisons between active setups and passive setups. Experiment 09 is a DMFC in completely active conditions and experiment 12 is a DMFC in completely passive conditions, while experiment 10 operates in active mode on the anode and passive mode on the cathode and experiment 11 operates in passive mode on the anode and active mode on the cathode. The major difference in OCP between experiment 09 and experiment 11 is due to an increase amount of methanol crossover from a higher concentration of methanol being used. DMFCs with liquid fuel have excess water from diluted methanol, which keeps the anode well humidified and allows more than sufficient water to react with the methanol when compared to concentrated vapor fuel. The low vapor pressure in the anode-passive fuel cell experiments and dependence on the water gradient between the anode and cathode reduced the vapor DMFC performance further at higher current densities. This was countered with the cathode-active forced air flow, removing water from the cathode reaction and reducing the concentration gradient, as demonstrated with experiment 11. Otherwise, excess water accumulated in the GDL on the cathode blocks oxygen access to the cathode catalyst (Eccarius et al., 2008).

	Anode			Cathode		
Experiment	Mode	Form	c_{MeOH}	Mode	λ	OR
Exp.09	Active	Liquid	0.5 M	Active	6	–
Exp.10	Active	Liquid	0.5 M	Passive	–	–
Exp.11	Passive	Vapor	50 wt%	Active	2	6.8%
Exp.12	Passive	Vapor	50 wt%	Passive	–	6.8%

Table 1: Experiment Labels for Figure 9 (Eccarius et al., 2008)

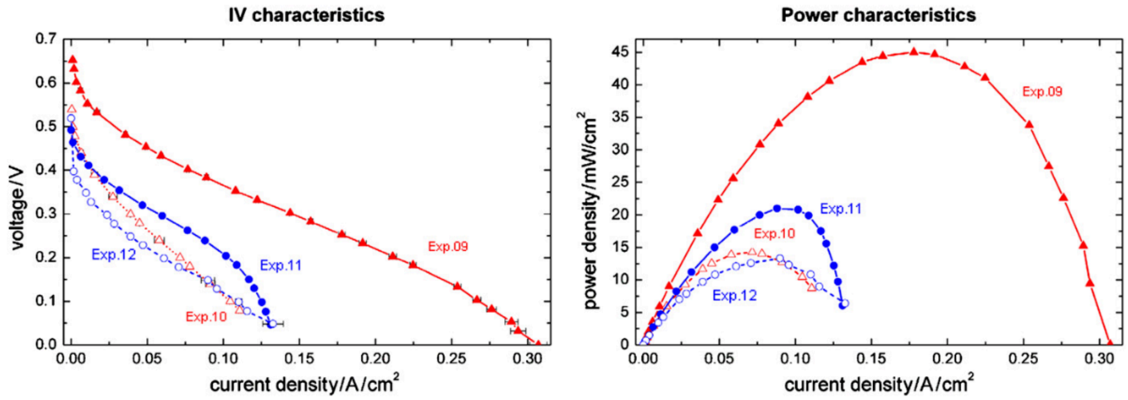

Figure 9: Polarization Curves Between Active and Passive Conditions (Eccarius et al., 2008)

Vapor Fuel Source

While liquid methanol is used as the fuel source in passive and standard DMFCs, a major issue with liquid fuel in passive DMFCs is the carbon dioxide buildup. As the fuel cell runs, carbon dioxide production in the anode GDL prevents access of methanol to the catalyst (Eccarius et al., 2008). Normally, this is less of an issue with in-flowing methanol feed. To counter this, vapor methanol has been proposed as an alternative due to its high volatility. Rather than supplying a continuous feed of methanol to the fuel cell, the methanol can instead be stored and supplied without heat to the fuel cell. Some advantages of vapor methanol over its liquid state include shorter start up times due to its greater mass diffusivity and higher temperature operations, which can increase reaction rates. There have been several successful runs with vapor feed DMFCs. Kim et al. (2006) developed a semi-passive DMFC which supplied methanol to a porous sponge and used a membrane that helped prevent a high level of methanol crossover and GDLs that were constructed from hydrophilic nano-materials, which helped force the water from the cathode back to the anode through the PEM. Overall, his results showed that the fuel efficiency for vapor methanol was 70% more efficient and had an energy density 1.5 times greater than that of liquid methanol. Shukla et al. (1997) was able to obtain a current density of 75 mA/cm^2 at 0.55 V with a vapor feed of 1% methanol and an OCP of ~0.9 V using a PEM electrolyte. Its performance improved with a vapor feed of 2M up to a current density of 100 mA/cm^2 at the same voltage.

While vapor feed DMFCs have potential, there are several issues that need to be researched more. According to Rice et al. (2007), in order to get promising results from vapor feed, the issue with water management must be resolved. While the DMFC is running and water is being produced from the reactions, water condenses on the anode GDL, causing the methanol concentration to decrease. This causes the methanol driving force into the anode GDL to decrease due to the water's inability to diffuse through the methanol fast enough. Rice also discovered that the water produced was greater than the water evaporated, being detrimental to the DMFC's performance (Rice et al., 2007). In the experiments run by Kim et al., polarization curves (Figure 10) were obtained after applying 1000 mA of current were for one hour in both a liquid fed passive DMFC and a vapor fed passive DMFC in order to exclude the effects of methanol and water accumulation on the OCP. While the vapor feed performed better at lower current densities due to less methanol crossover, the liquid feed had a better performance at higher current densities because of higher catalytic activity and a higher generated temperature. In addition, the vapor feed passive DMFC shows signs of mass transfer resistance at below 0.25 V, indicating that there were issues in transferring the fuel to the fuel cell.

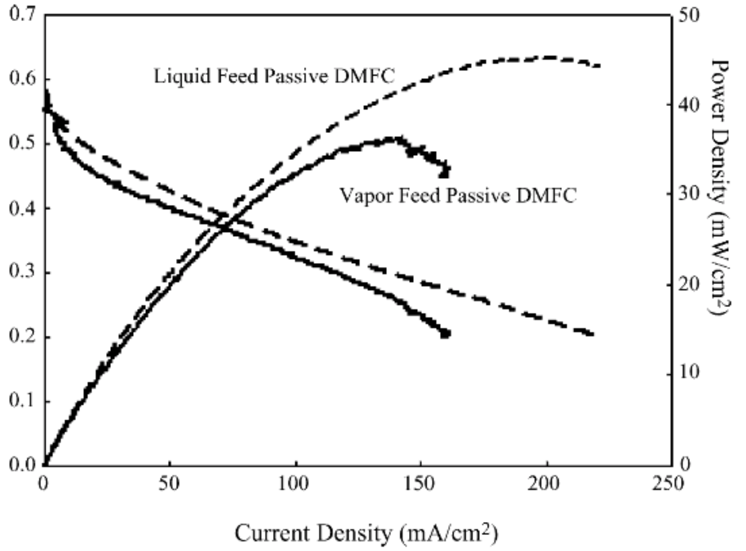

Figure 10: Feed Composition Comparison (Kim et al., 2006)

Feed properties

One of the largest issues in both standard and passive DMFCs is methanol crossover. Methanol crossover occurs when unreacted methanol on the anode is carried over to the cathode, resulting in a short circuiting current and hence causing a decrease in the overall fuel cell voltage as well as fuel loss. While standard DMFCs obtain a high power density at lower methanol molarities (1M or 2M), passive DMFCs can reach high power densities at higher molarities. Figure 11 shows the polarization curves of a passive DMFC at different methanol concentrations. At low current densities, lower concentrations give a higher voltage and OCP. However, Figure 11 also indicates that the maximum power density is attainable with 4M methanol, decreasing onward. The reasoning for this phenomenon is due to the passive fuel cell's reliance on diffusion of methanol, improving its mass transfer to the anode catalyst layer. A higher methanol concentration is also directly correlated to the operating temperature of a passive DMFC; a higher molarity leads to a higher permeation rate through the MEA, allowing more methanol to react with oxygen. Because the reaction on the cathode side is exothermic, the increase in reacting methanol will cause the operating temperature of the passive DMFC to increase. The increase in temperature, which speeds up the kinetics in the reacting methanol and oxygen, decreases the internal resistance, and therefore improves performance, in a similar fashion to standard DMFCs (Liu et al., 2005). It is important to note that there is no clear indication of the best methanol molarity due to the several variables that can affect the performance of a passive DMFC, including thickness, catalyst composition, and type of treatment (post-treatment versus pre-treatment). Bae et al., determined that the optimal power density was obtained at 5M (Bae et al., 2005).

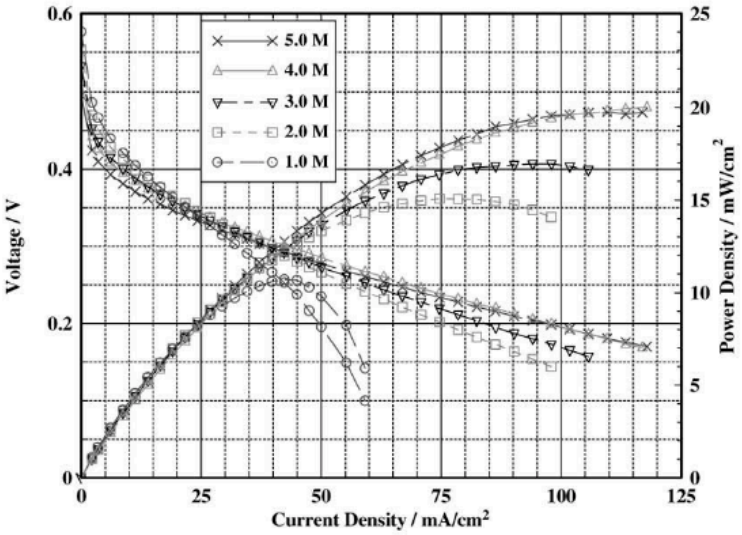

Figure 11: Methanol Molarity Comparison (Liu et al., 2005)

Temperature Variation

A major difference between passive DMFCs and active DMFCs is the operating temperature of the fuel cell. Temperature has a large influence on the electro kinetics of the reaction; with an increase in temperature, the ohmic resistance and activation resistance decreases (Jung, 2005). In a standard DMFC, the operating temperature is usually between 50ºC and 90ºC, whereas a DMFC in completely passive conditions operates at room temperature. Figure 12 shows a correlation with increasing temperature and the effect on performance; as the temperature increases, overall performance of the DMFC increases due to an increase in the electrochemical kinetics (Casalegno et al., 2007). While an increase in temperature usually improves performance, there are situations where a temperature increase is detrimental, depending on membrane thickness and molarity. Field's research shows that a temperature increase to an E-TEK MEA with

5M methanol decreases in performance at higher current densities. The reasoning behind the loss in performance is an increase in methanol crossover due to the weakening of the PEM. Chen mentions that at higher temperatures, the rate of methanol diffusion across the PEM may be higher than the catalytic efficiency, causing a decrease in performance (Chen et al., 2008).

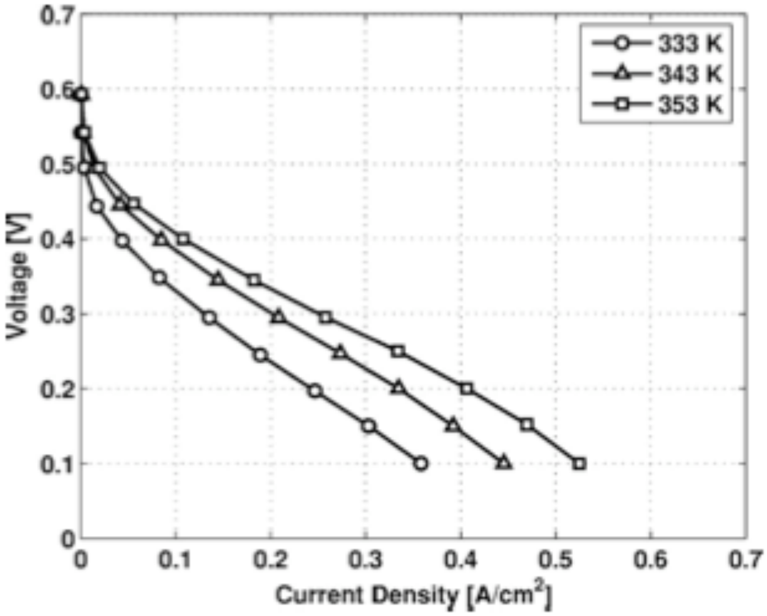

Figure 12: Polarization Curve With Varying Temperature (Casalegno et al., 2007)

Proton Exchange Membrane

Another parameter affecting the methanol crossover in both a standard and passive DMFC is the thickness of the PEM. Methanol crossover occurs from a combination of molecular diffusion and electro-osmotic drag. Molecular diffusion occurs at low current densities while electro-osmotic drag occurs at high current densities. Both thin and thick PEMs have advantages and disadvantages. A thicker PEM prevents methanol crossover better than a thinner PEM, providing better performance. However, a thinner PEM has a smaller internal resistance and allows the passive DMFC to operate at a higher temperature, which leads to better performance. Figure 13 shows the results of different polarization curves with varying thicknesses. At low current densities, the Nafion 117 performs the best, while the Nafion 112 performs the worst. Meanwhile, at higher current densities, the Nafion 112 performs better than the Nafion 117. This indicates that while Nafion 112 has a smaller internal resistance, improving performance at higher current densities, it also suffers from a larger amount of methanol crossover, which hinders its performance at low current densities. In the high current density region, the Nafion 112 membrane's smaller internal resistance becomes predominant in its performance. In addition, the methanol crossover rate becomes less of a factor at higher current densities, improving the Nafion 112 performance further.

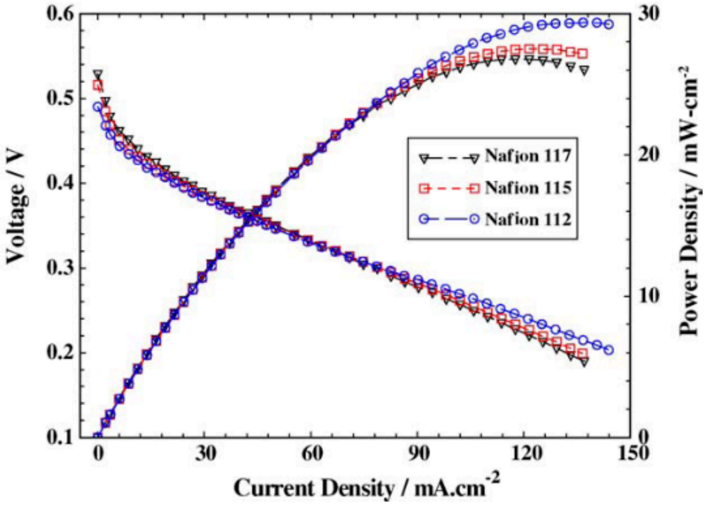

Figure 13: PEM Thickness Comparison (Liu et al., 2006)

Cathode GDL

The cathode GDL is responsible for supplying the oxygen to the cathode catalyst layer for reacting oxygen with the incoming electrons provided from the anode or the methanol directly, and produces water and heat. In passive DMFCs, because oxygen is replaced with ambient air, its performance is affected significantly by the lack of oxygen provided and water flooding in the cathode GDL. These issues prevent mass transport and increase the mass transfer resistance (Chen et al., 2006). This ultimately effects the efficiency of the fuel cell; a DMFC relying on ambient air has half the total efficiency of a DMFC with forced air flow (about 6% versus about 11%) (Eccarius et al., 2008). To resolve this issue, Chen proposed a new MEA with the cathode GDL removed; with the removal of the cathode GDL, the new MEA will allow a higher oxygen transfer rate, providing better performance. Although early indications of the cathode GDL removal showed an increased resistance, this was primarily due to the increased gap between the cathode catalyst layer and the current collector. When testing 4M methanol, tests showed (Figure 14) that the new MEA performed slightly better than a conventional MEA at zero voltage and low voltage. This increase was due to the increased oxygen transfer rate at high current densities, which improved the kinetics of oxygen reduction. The difference in performance is more apparent at higher voltages. With the higher requirement of oxygen at a higher molarity due to the increased methanol crossover, oxygen could be consumed more readily. As a result, the mass transfer resistance decreased dramatically. The IR correction indicates more accurate results. Long-term performance, on a transient discharging voltage with a constant current density between the two MEAs, was also performed. A conventional MEA was shown to have a bigger and more rapid decrease in OCP than a new MEA due to the increase oxygen transfer rate and decreased flooding.

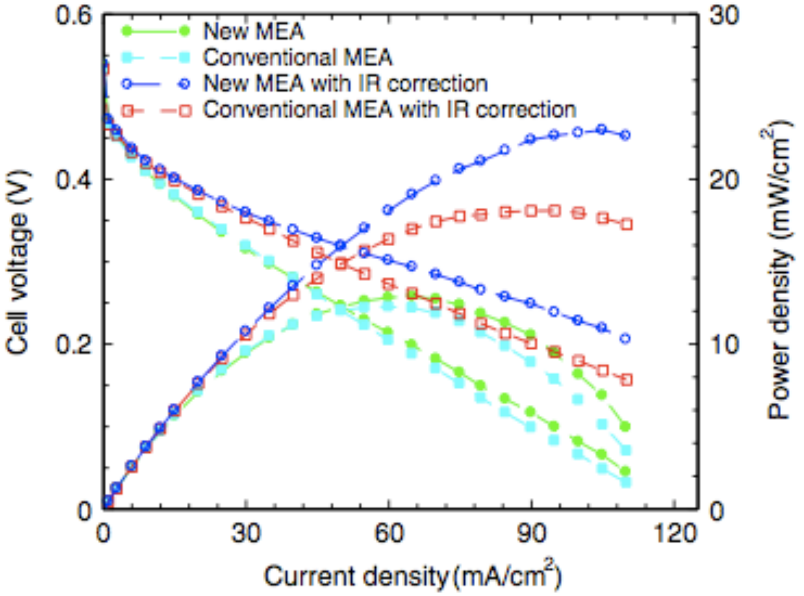

Figure 14: New MEA Versus Conventional MEA Performance (Chen et al., 2006)

Current Collectors

Several modifications to the current collectors have been proposed to increase the performance of passive DMFCs. A proposed method was the use of a porous current collector on the cathode as opposed to a perforated current collector. The porous construct facilitates the flow of oxygen and water transport. In addition, because the heat generated from the cathode GDL is lost within the cathode current collector, diminishing the performance of the fuel cell, a current collector with a low thermal conductivity is also important. Other important features in a current collector include high electrical conductivity, good mechanical strength, and a uniform transport area. Chen's results showed that porous current collectors have a better performance at higher current densities while perforated current collectors have a better performance at lower current densities. In addition, the porous current collectors provided a higher cell temperature, allowing for easier proton transport, supporting the experimental evidence of improved performance. In addition, a smaller particle size in the porous current collector decreases the cell resistance, improving performance further (Chen et al., 2007). During Shimizu's testing of micro passive DMFCs, a test was run on two different current collector materials: a stainless steel mesh and a gold-plated stainless steel mesh. According to Figure 15, Shimizu's results indicate that the gold plated stainless steel mesh performed better than the stainless steel mesh due to the gold's higher conductivity (Shimizu et al., 2004). While there is no indication whether the thickness of the current collector has an effect on passive DMFC performance, thicker metals will last longer than thinner metals due to a metal's corrosion rate. Stainless Steel 316 (SS316) in direct contact with methanol has a corrosion rate (rate at which corrosion penetrates the metal) of 0.002" per year independent of amount of water and temperature while a brass alloy has a corrosion rate of 0.020" per year (De Renzo, 1985). However, SS316 has a relatively low electrical conductivity (Oberg et al., 2000).

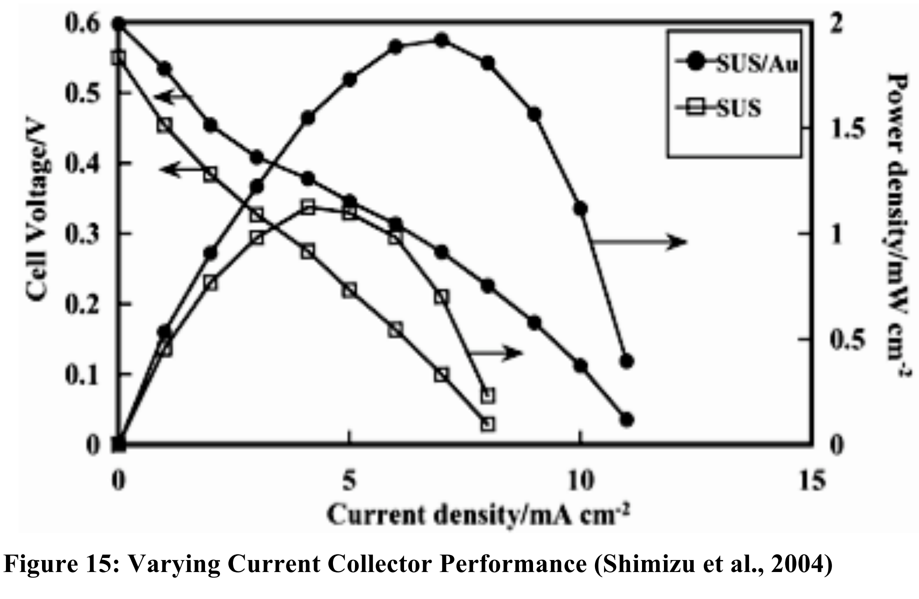

Figure 15: Varying Current Collector Performance (Shimizu et al., 2004)

Methodology

The purpose of this project was to design and construct a passive DMFC with the capability to power a portable electronic device, such as an iPod. Developing the passive DMFC required several different aspects, including assembly of the fuel cell, preparation and fabrication of the MEA, and testing of the fuel cell as well as several MEA variations. In addition, a toy car supplied with methanol as a fuel was also tested to observe the performance of a passive DMFC under several different conditions.

Preparation and Fabrication of Membrane Electrode Assembly

The PEM used was a Nafion membrane obtained from ElectroChem, Inc. More specifically, the Nafion membrane, manufactured by DuPont, is a transparent non-reinforced film based on Nafion PFSA polymer, a perfluorosulfonic acid/PTFE copolymer in acid form. The thickness of the Nafion membrane used was one of the following:

- Nafion membrane N1035, (1000EW, 3.5 mil thick)
- The EC-NM-115 N115 membrane (1100 EW, 5 mil thick)
- Nafion membrane N117 (1100 EW, 7 mil thick)
- Nafion membrane N1110, (1100EW, 10 mil thick)

The Nafion membrane was cut into 5 cm by 5 cm squares with scissors. Using tweezers, 1-2 Nafion membranes were inserted into a Pyrex® beaker with deionized water at a low boil for about an hour. The Nafion membranes were then transferred to a beaker with 3 wt% hydrogen peroxide for 1.5 hours at a low boil. The hydrogen peroxide oxidized the organic purities within the Nafion membranes. Following the hydrogen peroxide treatment was another hour of deionized water at a low boil, then 1.5 hours in 0.5 M sulfuric acid at a low boil. The sulfuric acid protonates the sulfonic acid sites in the Nafion, allowing proton transport to occur. Afterwards, the Nafion membranes were once again submerged in deionized water at a low boil for another hour. It was critical to maintain a low boil throughout the entire process; rapid boiling causes damage to the membrane surface.

After preparing the Nafion membranes, they were pressed with Kim Wipes in the Carver hot press (Figure 16) without heat or excess force for five minutes. This was done to flatten out the Nafion membranes and ease the process of the electrode addition. After the Nafion membranes were pressed, the Carver hot press was heated up to 275ºF. While the hot press heated up, the anode and cathode electrodes were cut into 2 cm by 2 cm strips and carefully aligned on the back and front of the Nafion membranes with one of the sides clearly labeled in a corner of the membrane with a Sharpie. The Nafion membranes, along with the anode and cathode electrodes, were sandwiched by two Teflon sheets and then placed in the hot press for two minutes with an applied force of two tons. After that time, the newly created MEAs were allowed to cool for 10 minutes before being properly stored for future use. When higher voltage was required to test the home-made fuel cell, the electrodes were cut into two or three 2 cm by 1 cm strips instead about 3/8’’ from each other.

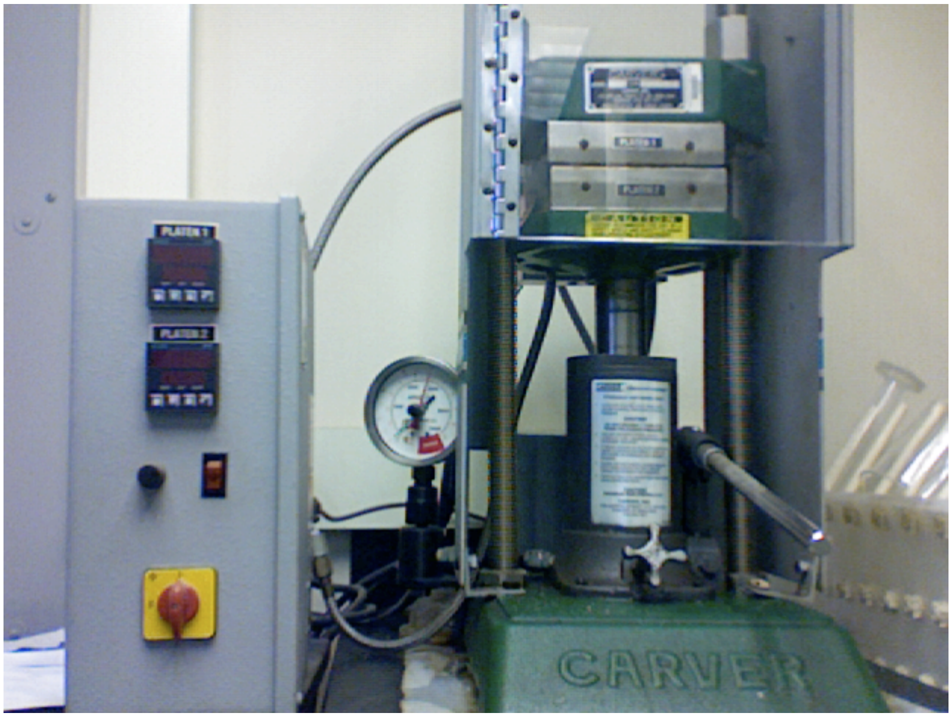

Figure 16: Carver Hot Press

Ordered Components of the Fuel Cell MEA

In order to test the optimal performance of the DMFC, toy car, and home-made fuel cell, an E-Tek, Inc (a subsidiary of BASF Fuel Cell, Inc.) commercial MEA was purchased. The MEA, model ES12D-W-5L, is a five layer assembly, two electrodes, two catalyst layers, and a PEM, using woven web as the material in the GDLs and advanced ELAT® carbon cloth flow fields. While the exact composition of the catalyst is not known, it has been constructed with Selectra® high performance catalysts. It is important to note that despite heavy use and deformation, this MEA still performs very well.

In addition, several commercial MEAs were also purchased from Clean Fuel Cell Energy (Figure 17). The MEA is a custom model with an electrode size of 5 cm^2. The catalyst on the anode has a loading of 4 mg $PtRu/cm^2$ and the cathode loading is 4 mg

Pt/cm^2. The PEM is a 117 Nafion membrane about 5 cm x 5 cm. The properties of the GDL are unknown.

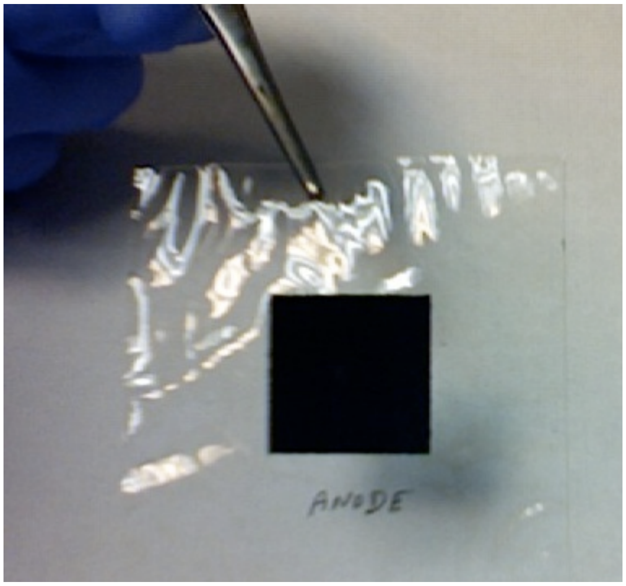

Figure 17: Clean Fuel Cell Energy MEA

Due to the unsuccessful attempts at preparing home-made catalysts, electrodes were also purchased from ElectroChem, Inc. The anode electrode was an EC-Electrode-C1, an EC-40-60-PtRu-C electrode with a catalytic layer containing 40wt % Pt/C and 20 wt% Ru/C and a loading of 4 mg $PtRu/cm^2$. The GDL used in the anode electrode is a carbon cloth with a Nafion coating. The cathode electrode was an EC-Electrode-C2, an EC-40-40 Pt-C electrode with a catalyst layer of 40 wt% Pt/C and a loading of 4 mg Pt/cm^2. The cathode GDL used is the same material as the anode GDL.

Passive DMFC Toy Car

To test an already working passive DMFC, the hydro-Genius Desk Top Model Car was utilized (Figure 18). The toy car comes with an already assembled fuel cell setup, including a compartment to hold liquid methanol in contact with the anode electrode, two perforated stainless steel current collectors, and an MEA provided by the company. Two rubber plugs are used to prevent methanol vapor from escaping the methanol compartment. The back of the fuel cell allows ambient air to diffuse to the cathode electrode. While the composition of the catalysts, anode GDL, and membrane are unknown, the toy car's cathode GDL is replaced by a piece of carbon paper. Using the supplied 2% methanol solution, the toy car can power its motor attached to the wheel, which is controlled by a power switch on the cathode current collector. According to the manual provided by the company, the toy car MEA needs to be in contact with the methanol for about 10 minutes before the motor can run successfully. The toy car was modified with the addition of alligator clips in order to provide a more stable connection to the fuel cell station. For voltage testing, a Wavetek voltage reader was used.

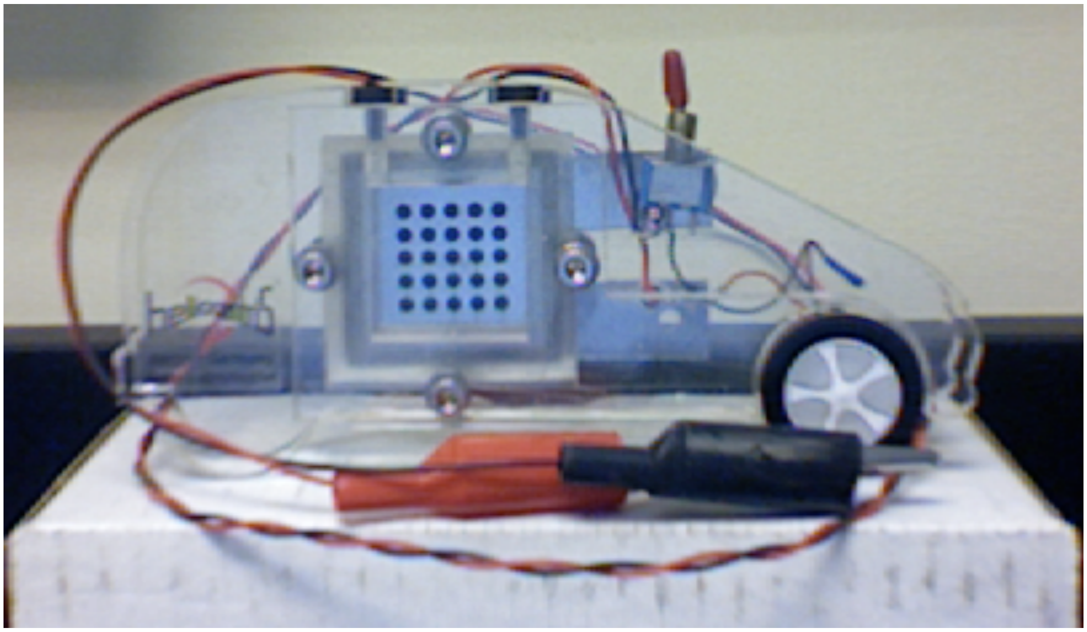

Figure 18: Hydro-Genius Desk Top Model Car

Fabrication of the Home-made Fuel Cell

The fuel cell box-structure was machined from a block of acrylic. Figure 19 shows a basic schematic of how the fuel cell was constructed. The dimensions of the fuel cell were cut into about a 3” x 3” x 3” cube with its core cut out for the methanol storage, a screw-in top plate to prevent methanol vapors from escaping as well as air vapors from entering, its four sides with a 2 cm by 3 cm opening cut out to allow the methanol to be in contact with the anode-side MEA placed over the opening, and screw-in sides to firmly seal and retain the current collectors, MEA, and gaskets. The OCP, voltage versus current density, and voltage and power density of the home-made fuel cell was tested with different MEA thicknesses, methanol molarities, current collectors, and gaskets. For comparison, Field’s (2008) results of testing the different properties, including MEA thickness and methanol molarity, were used as a reference.

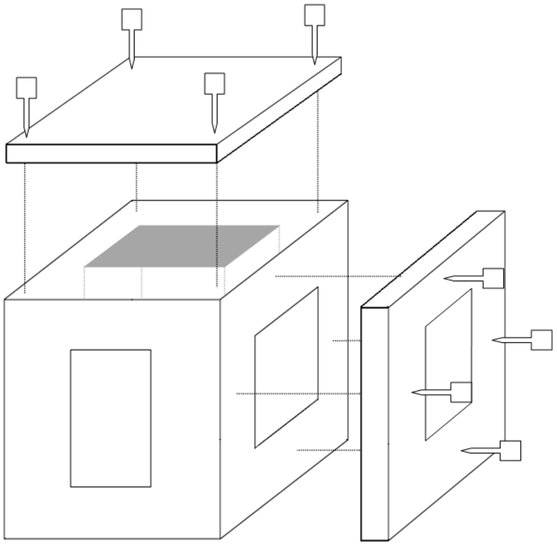

Figure 19: Schematic of the Fuel Cell Design

The current collector Materials Of Construction (MOC) tested in the home-made fuel cell was perforated SS 316 with a thickness of 0.018”. All current collectors were cut to about 2” by 1 5/8” with a small tab to allow wiring between current collectors and a proper connection to the electronic load box. The center of the current collector was cut into 1/8” holes expanding a square area of 3/4” by 3/4”. The current collectors were supplied by OnlineMetals. The MOC for the gaskets included: silicone, and Teflon. All gaskets were cut to the dimensions of the fuel cell with a hole the same size as the opening in the fuel cell. The Teflon was placed between the current collector and MEA and the silicone was placed between the fuel cell and anode current collector.

Figure 20 represents a circuit diagram of the home-made fuel cell setup with four single cells (MEAs) connected in series. Because four MEAs will be connected in series, the voltage obtained will be cumulative. In theory, if all four MEAs can supply at least 0.375 V, the passive fuel cell will have similar properties to one battery, which typically supplies 1.5 V. Once the passive fuel cell had the capability of a battery, it went through long term testing to calculate the capacity and efficiency by measuring power and current with respect to time.

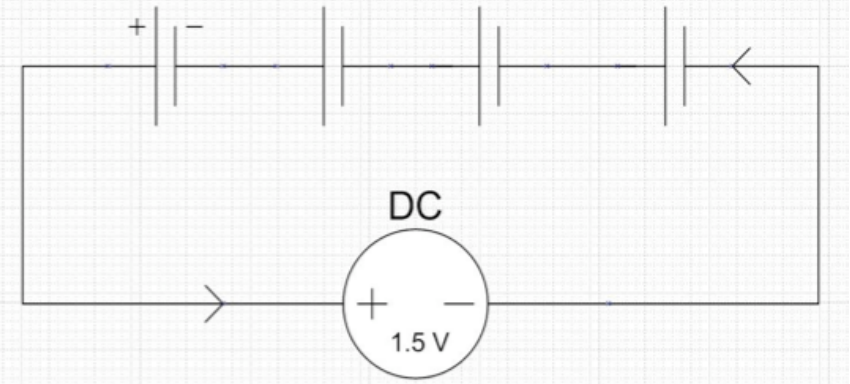

Figure 20: Circuit Diagram of the Home-Made Passive DMFC

Figure 21 and Figure 22 show an active conventional single-cell DMFC labeled with the path flows of methanol and the constructed passive DMFC. The active DMFC requires multiple pieces of equipment to run, including a methanol pump, an oxygen tank, and additional tubes to direct the flow of methanol and oxygen into and out of the cell. Meanwhile, the passive DMFC does not require any additional equipment. In addition, as long as there is methanol in its reservoir, the passive DMFC will run. Because of this, there is an immediate conclusion that a passive DMFC will be much more convenient in portable devices over an active DMFC, and without the parasitic losses of ancillary equipment, albeit the performance is expected to be larger.

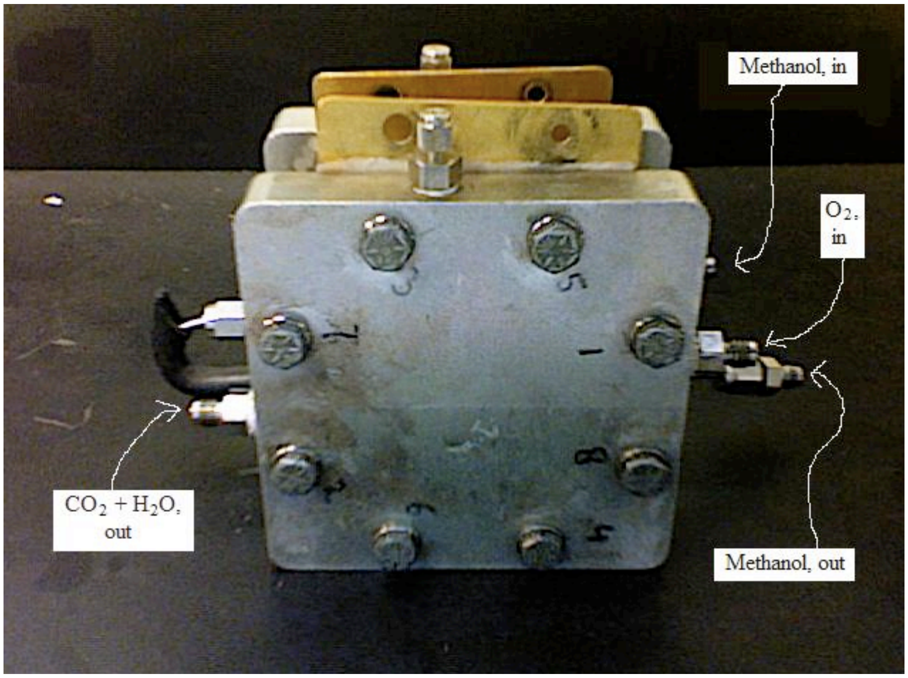

Figure 21: Active DMFC, Flow Paths Labeled

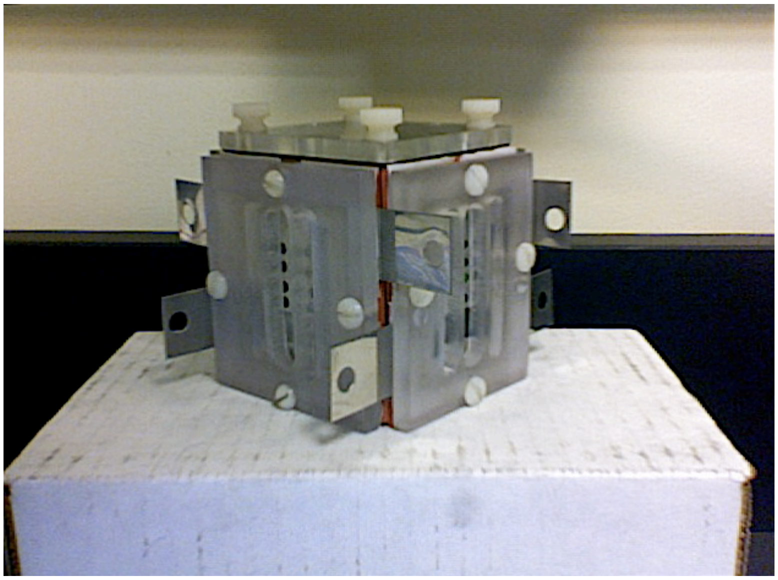

Figure 22: Home-made Passive DMFC

Testing the MEA

All three types of fuel cells, a DMFC with the home-made MEA, the toy car, and the home-made fuel cell, were all tested in a fuel cell testing station, which included a setup for supplying methanol and oxygen to the DMFC as well as a Hewlett Packard electronic load box model 6060B (Figure 23).

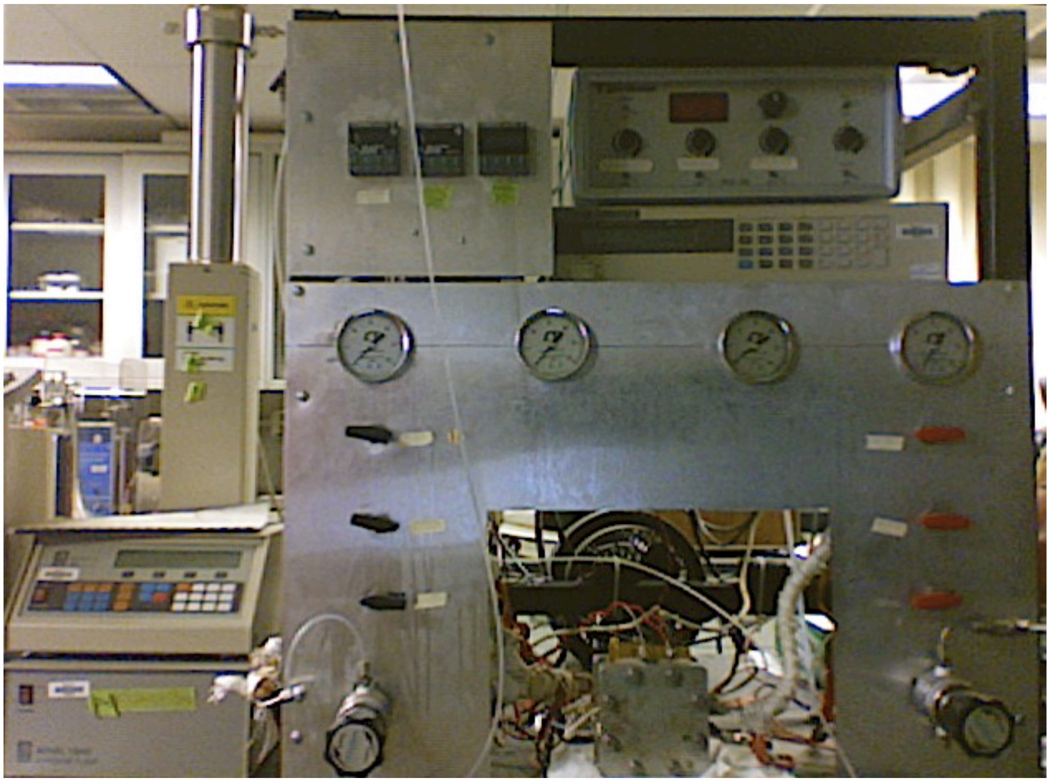
Figure 23: Fuel Cell Testing Station

To test the MEA, it needed to be assembled between two bipolar plates. The MEA was first placed on a cell bipolar plate, with a gasket above and below the MEA. Carefully, the second bipolar plate was placed on top and screwed in. The bipolar plates were then bolted in, first with 60 in-lbf of torque and again with 65 in-lbf of torque. It is crucial to prevent the bipolar plates from moving to avoid the MEA from shifting its position. Once the DMFC is set up, it was then hooked up to the fuel cell testing station. Tubes from the methanol pump and oxygen tank were screwed into the inlets while waste tubes were connected to the outlets. Heating elements were placed inside the fuel cell to heat it up to the desired temperatures. The anode electrical wiring (black wire) and cathode electrical wiring (red wire), were connected to the fuel cell current collectors on the anode side and cathode side respectively. The aqueous methanol flow in the anode bipolar plate was set to 1 mL/min white the oxygen flow to the cathode bipolar plate was maintained at 70 mL/min. In the case that methanol vapor was used as the feed, methanol was poured into a flask and plugged up by a rubber stopper containing a tube connecting to the DMFC. The temperature of the fuel cell was set to 70ºC and the humidifier temperature for oxygen was set to 35ºC. Once the load box was switched on, the fuel cell ran between 10-30 minutes before the OCP stabilized. Afterwards, the load box was set to 0.2 V and allowed to stabilize for 4-6 hours, or until the displayed current had not changed for an hour (indicating stability). Once the fuel cell stabilized, the current was recorded at different voltages varying between 0.2-0.6 V. Because the load box was not designed to test at such low voltages, 0.1 V readings were not recorded.

Due to the hard to access current collectors in the toy car, extra wiring was required to set up the toy car to the fuel cell testing station. When a home-made MEA was to be tested, the toy car was disassembled and the toy car MEA was replaced with the home-made MEA. The procedure in which the data was recorded is the same as that for the DMFC.

The home-made fuel cell was connected to the fuel cell testing station by the current collectors. The methanol supply was stored and sealed in the inside reservoir. In the case that only one side of the home-made fuel cell was tested, the other three sides were replaced with a layer of silicone to prevent the methanol liquid/vapor from escaping. When all four sides of the home-made fuel cell were tested, the current collectors were connected with a stainless steel wire, leaving an anode current collector and a cathode current collector exposed. The process in which the data was recorded is the same procedure as the active DMFC. The fuel source used in the home-made fuel cell varied between liquid methanol, methanol stored in a beaker inside the compartment relying on the ambient vapors, and methanol chafing gel (Figure 24). The methanol gel is similar to Sterno that is commonly used to heat prepared foods in chafing dishes for up to two hours. The methanol gel was obtained from WPI's Goat's Head Pub and was manufactured by Candle Lamp Company (See Appendix IV for MSDS details). Its composition is shown in Table 1; while not listed, it is assumed that the methanol gel contains about 25 wt% water.

Figure 24: Methanol Chafing Gel

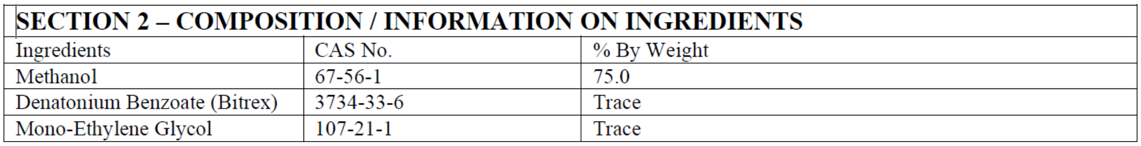

SECTION 2 – COMPOSITION / INFORMATION ON INGREDIENTS		
Ingredients	CAS No.	% By Weight
Methanol	67-56-1	75.0
Denatonium Benzoate (Bitrex)	3734-33-6	Trace
Mono-Ethylene Glycol	107-21-1	Trace

Table 2: Composition of Methanol Chafing Gel

The concept of using methanol gel is a fresh idea and has only been mentioned in a few patents. According to Patent No. 5773706, a gelled organic liquid has a slower rate of evaporation, thereby increasing its effectiveness. Also mentioned is nitrocellulose as a gelling agent for fuels such as methanol. However, the gel can separate from the methanol, creating an undesirable product. Other better alternatives include using "carboxyl vinyl polymers neutralized with a weak amine base" and Carbopol 934 (Wesley et al., 1998).

Mass Academy High School Student Assistant

This work was done in collaboration with Ashley Millette, a student from Mass Academy High School. Mass Academy High School, a WPI-affiliated school specializing in teaching advanced mathematics and science through "teach yourself" methods, is a high school for 11th and 12th graders with a class of about 50 students per grade. The 11th graders are required to complete a project, which can span up to six months, and show their work at their science fair. Of the class of 46 (as of 2009), only 12 students are selected to present their work at the regional science fair and possibly the state fair.

The student I worked set a goal to construct a passive DMFC that had enough power to run a 3rd generation iPod nano made by Apple. The 3rd generation iPod nano battery requires 3.7 V and 630 mAh to run (Apple, 2009). For eight hours of battery life, the passive DMFC with an active area of 5 cm^2 must produce about 16 mA/cm^2 of current density. Further, to achieve the stated voltage, one would need roughly 10 cells in series, or appropriate electronics to manage their power.

In addition to constructing the passive DMFC, it was also important to ensure that the Mass Academy student had a full understanding of the concepts behind fuel cell technology. This included the fabrication of the MEA, optimal builds for the fuel cell, discussion of successful reports from journals previous reports completed from WPI, and review of the results obtained from the home-made passive DMFC and toy car testing.

Results and Discussion

Several different experiments were conducted to determine performance characteristics of the different DMFCs under different conditions and with different feeds. First, different fuels, liquid methanol and vapor methanol, were tested and compared in an active DMFC. The toy car MEA was then analyzed in both an active and passive DMFC. Afterwards, the Clean Fuel Cell Energy MEA was tested with liquid methanol, first in the active DMFC setup, then in the home-made passive fuel cell setup (one side only). Vapor fuel was then tested in the home-made passive fuel cell setup (one side only), in addition to methanol chafing gel, and compared to the performance of liquid fuel. Working off an innovative idea, methanol gel was used as a primary fuel source to power a clock and a toy motor. Long term testing was also included to determine the capacity and efficiency of the passive fuel cell. The performance of a battery was also determined for comparison. All solid lines in the all graphs indicate the left axis and all dashed lines indicate the right axis.

Liquid Versus Vapor Feed

To test the efficacy of the fuel source used in the passive fuel cell, in addition to the information gathered from Field’s results, the effect of the state of the methanol feed was tested. The methanol was either fed as liquid methanol through a pump or as vapor methanol through a tube. Figure 25-28 show the results of the liquid and vapor feeds with different parameters. The molarities used were 3M and 5M and the membranes of variant thicknesses used were Nafion 1035 and 115. All tests were performed at 70ºC. When the concentration of methanol was increased for Nafion 1035, the performance of the vapor feed decreased both at high current densities while the performance of the liquid feed increased overall. With the Nafion 115, the increasing methanol concentration hindered the performance of both the liquid and vapor feed at high current densities. However, the vapor feed was affected more than the liquid feed. In addition, at lower current densities, the vapor feed performed better. When testing vapor fuel with high vapor concentrations, although performance was expected to be better, no current was obtained.

Normally, DMFC MEAs can provide a current density up to 100 mA/cm^2 at lower voltages. However, the electrodes ordered from ElectroChem, Inc. could not perform as well as anticipated. Because of this, the ElectroChem electrodes were not used in the construction of the home-made fuel cell.

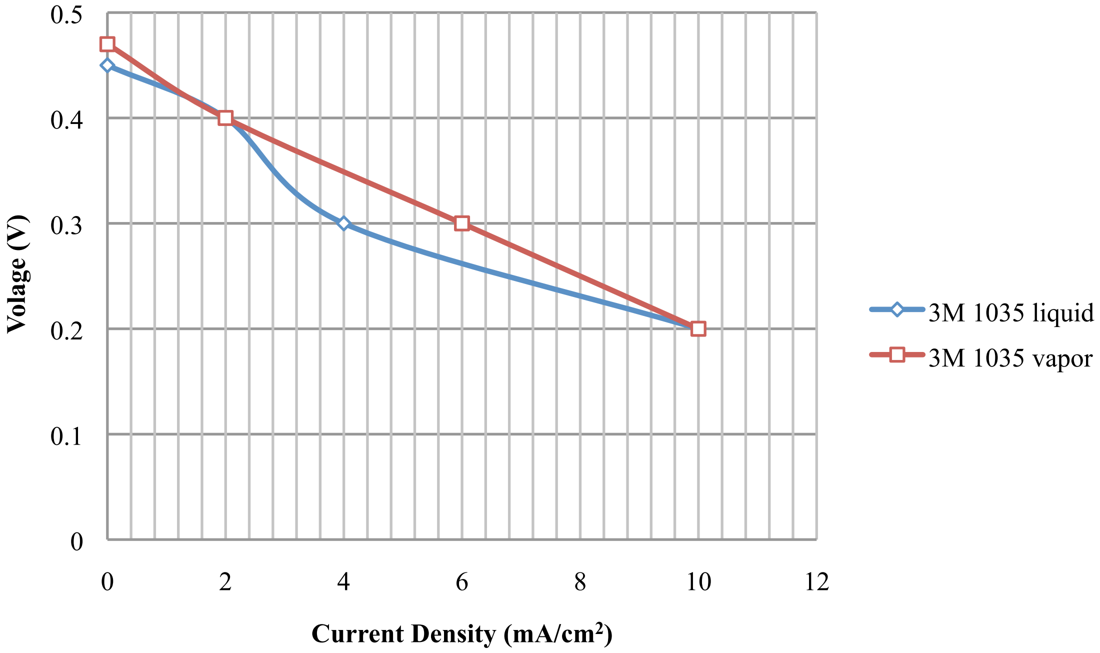

Figure 25: Feed Composition Comparison Test 1; Electrochem Inc. Electrodes

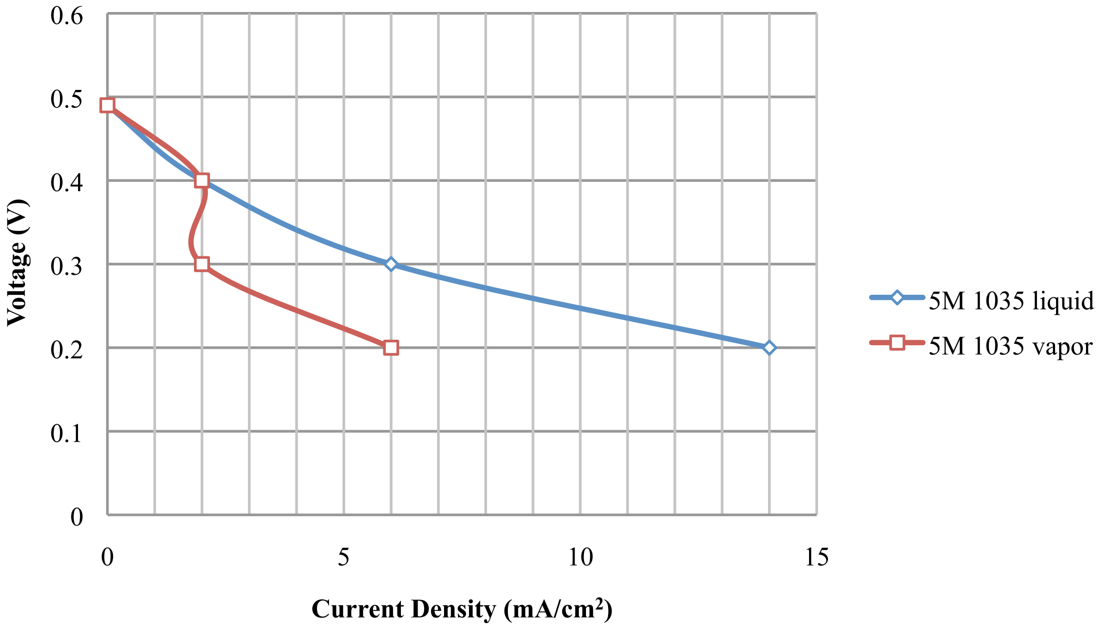

Figure 26: Feed Composition Comparison Test 2; ElectroChem Inc. Electrodes

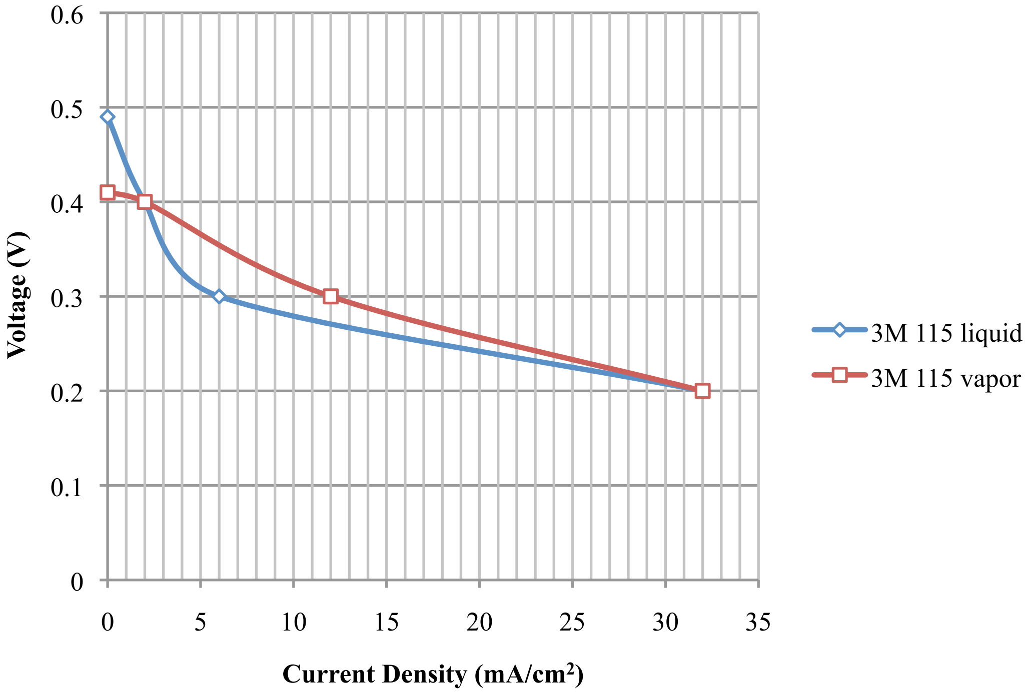

Figure 27: Feed Composition Comparison Test 3; ElectroChem Inc. Electrodes

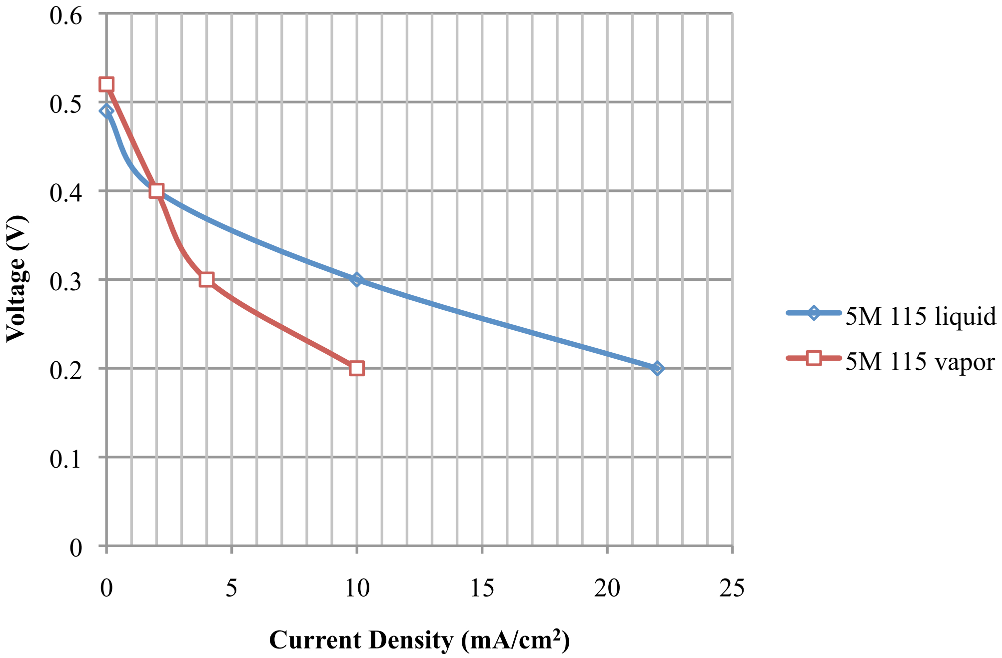

Figure 28: Feed Composition Comparison Test 4; ElectroChem Inc. Electrodes

Toy Car Testing

Figure 29 represents the polarization curve of the toy car's MEA in an active DMFC at 70°C with three different molarities (1M to 5M). At low current densities, the 1M methanol had the highest voltage while the 5M had the lowest voltage. At high current densities, 1M and 3M methanol performed similarly while the 5M methanol had the worst performance. Because the toy car was packaged with 3% methanol (just under 1M methanol), it is likely that the toy car MEA performs best with lower concentrations of methanol. Although the overall performance was better than the ElectroChem electrodes, it is still not up to par with standard MEAs. One reason for its poor performance could be the use of carbon paper on the cathode side. While that is a preferable attribute in passive fuel cells, it only diminished the overall performance. When testing the toy car MEA in the toy car, while providing a nice variety of different

OCPs with different parameters (see Appendix V), it either produced zero current or very little current (0.01 A at nearly zero voltage). Because of this, testing in the toy car was abandoned. For future testing, the toy car will make a suitable control experiment for liquid fuel.

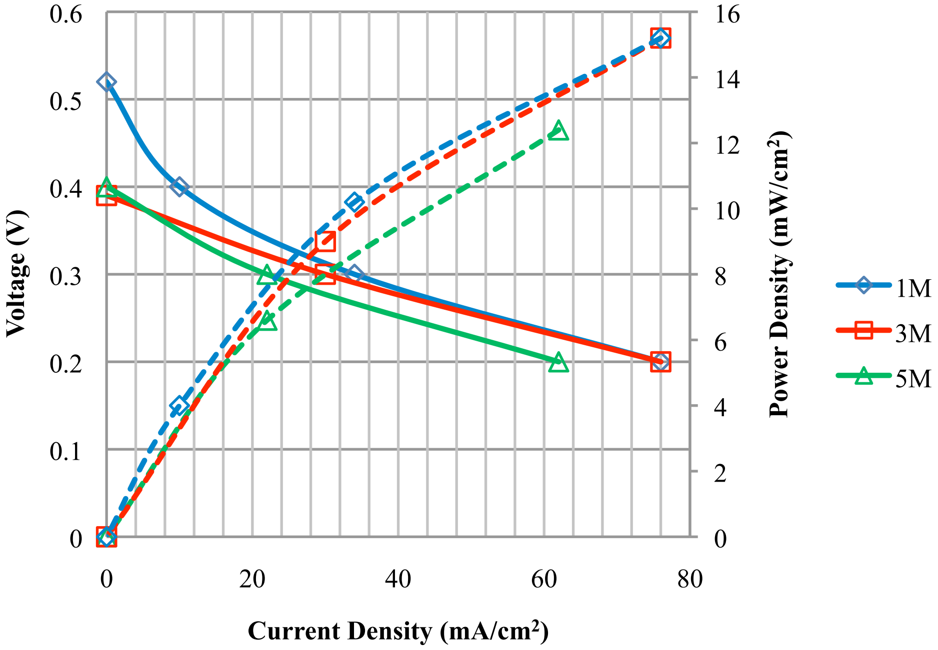

Figure 29: Toy Car MEA Polarization Curve

Clean Fuel Cell Energy MEA

Because of the poor performance of the ElectroChem electrodes as well as the home-made MEAs, commercial MEAs were ordered from Clean Fuel Cell. Before testing them in the home-made fuel cell, polarization curves were obtained in an active DMFC with varying methanol concentrations and a constant temperature of 70ºC. The results are represented in Figure 30, displaying both the voltage and power density with respect to current density. At low current densities, the lower molarities show the highest performance. As current density increases, the 1M is overtaken by the 3M, which performed the best out of all four concentrations, while the 7M performed the worst both at low and high current densities. The power density, obtained by multiplying the voltage and current density, is also plotted. Similar to the voltage-current density curve, the 3M methanol provided the highest power density (36 mW/cm^2) while the 1M and 5M methanol both give about the same power density, about 25 mW/cm^2.

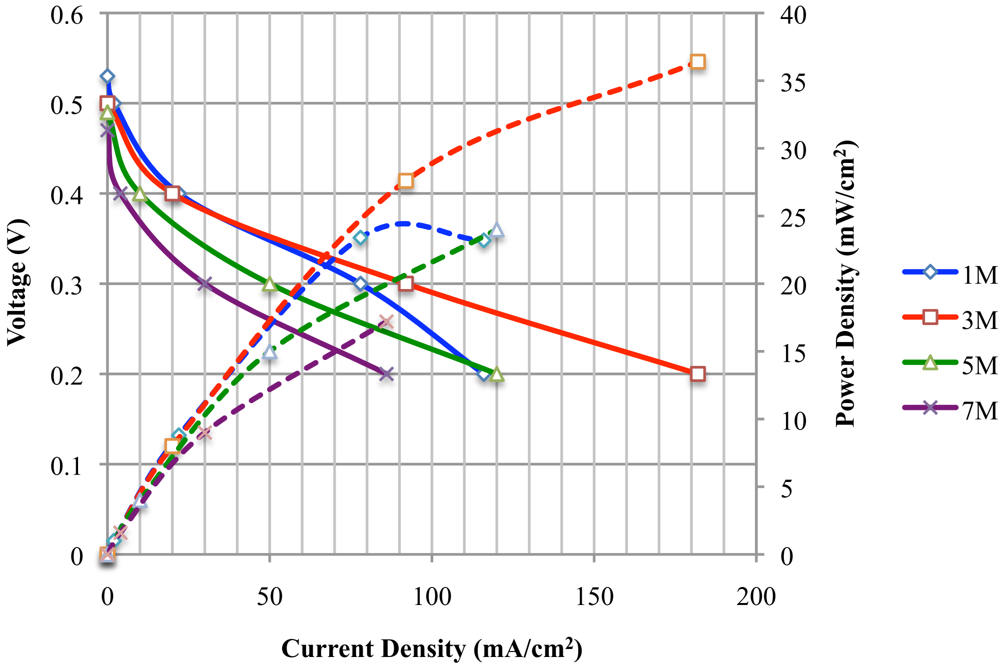

Figure 30: Polarization Curves in Active DMFC, Liquid Fuel

Home-made Passive Fuel Cell Testing

Figure 31 and Figure 32 indicate only one side of a passive home-made fuel cell being tested with liquid and vapor fuel, respectively. When the current densities of both figures are compared to the active fuel cell testing, it is clear that the passive fuel cell performs nowhere near as well as an active DMFC, both at high current densities and low current densities, the performance roughly being only a fifth of that in the active mode

In Figure 31, the lower concentrations of methanol perform slightly better than the higher concentrations at low current density and OCP conditions. At higher current densities, the 5M methanol outperforms the other concentrations while the 1M performs the worst. The 5M methanol also provides the highest power density by a decent margin, about 4 mW/cm^2.

In Figure 32, because vapor fuel was used, only 50% concentrated methanol and pure methanol were tested, in addition to methanol gel. Compared to the liquid fuel source in the passive fuel cell, overall performance diminishes primarily in the low current density region while the high current density region was not affect very much. This is likely due to the increase in methanol crossover from the use of a higher concentration of methanol. The 50% methanol solution performed nowhere near as well as the pure methanol fuel and methanol gel fuel, both at low and high current density regions. This shows that if enough water vapor is produced, the performance of the fuel cell may be reduced. Although pure methanol performed better at high current densities and provides a higher power density, the methanol gel produced a higher OCP and still provided a decent amount of power, about 3 mW/cm^2 at about 22 mA/cm^2.

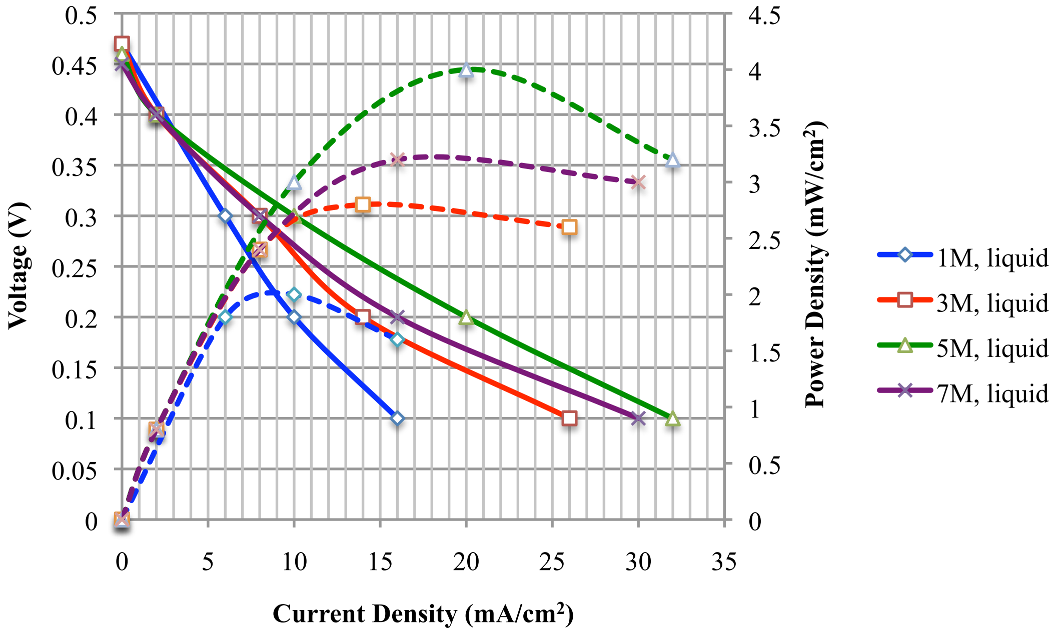

Figure 31: Polarization Curves in Passive DMFC, Liquid Fuel

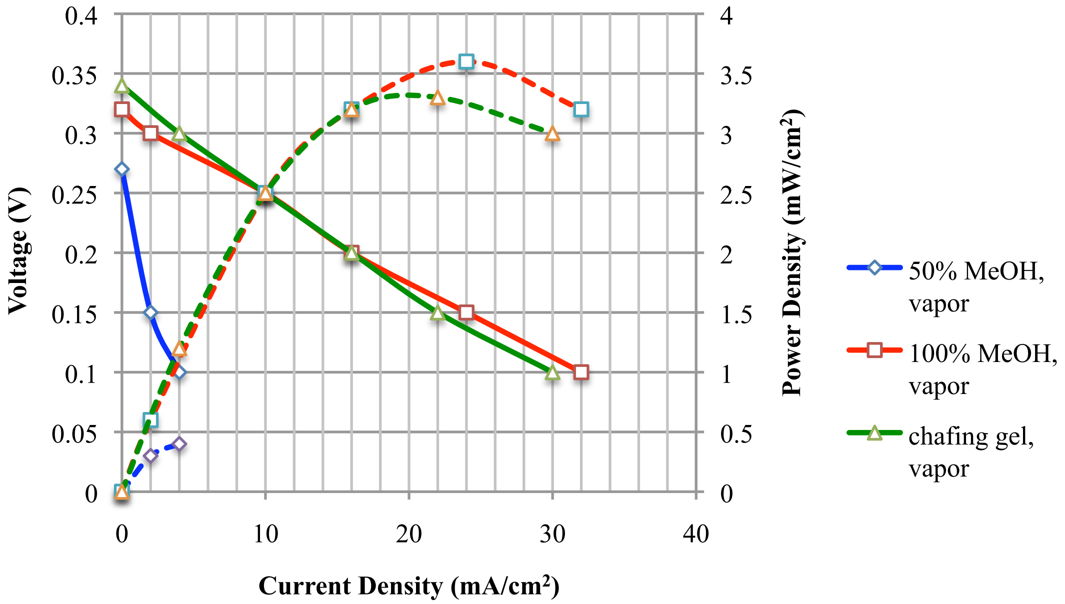

Figure 32: Polarization Curves in Passive DMFC, Vapor Fuel

Fully Assembled Home-made Fuel Cell

Once the passive fuel cell testing was completed, the three inactive sides were replaced with an MEA each and a series connection was made between all four MEAs. Figure 33 represents the polarization curve of the passive home-made DMFC with four MEAs electrically connected in series with methanol gel used as the fuel source. As anticipated, the voltage between the four MEAs did stack. However, the obtained OCP was higher than expected, reaching just over 1.6 V. Because current stays constant between the four MEAs, current density remained nearly unchanged. The overall increase in voltage still had an effect on the power density, increasing to about 13 mW/cm^2 at about 21 mA/cm^2.

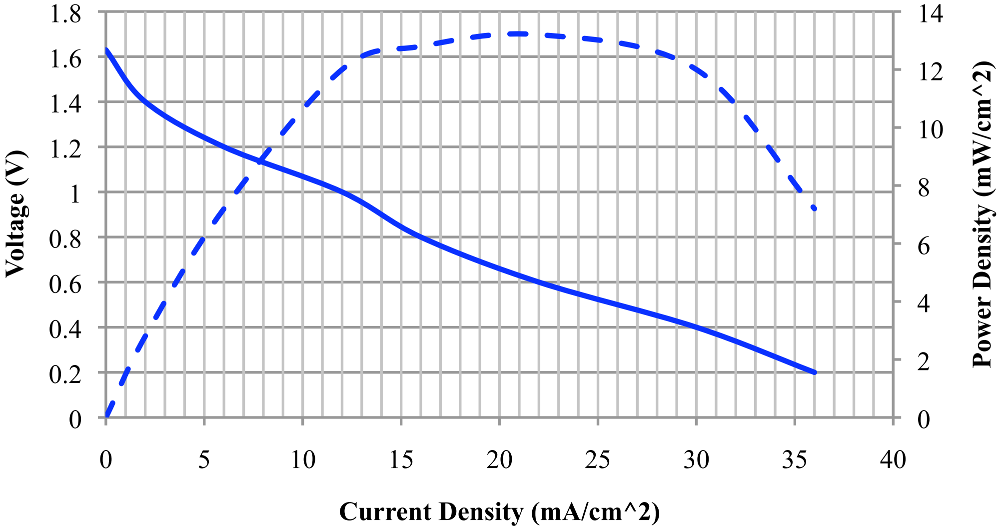

Figure 33: Polarization Curve for Fully Assembled Passive DMFC, Methanol Gel

The exceptional performance of the home-made passive fuel cell allowed for conventional use as a battery. Early testing was done to ensure that the fuel cell could work as a battery. Figure 34 shows the fuel cell connected to both the Wavetek voltage reader and a Radio Shack Travel Alarm Clock, using methanol gel as the fuel source (bird's eye view of the fuel cell). The smooth operation of to the clock proves that the home-made fuel cell does have the capability of replacing one 1.5 V battery. Long term testing was not performed with the clock due to the low current density requirements of the clock; fuel is exhausted more quickly when a higher current is required to power a device, such as a motor. Based on the voltage reading in Figure 34, the clock required less than 2 mA/cm^2 of current density. An interesting observation is the decomposition of the methanol gel; as the fuel source is being consumed by the MEAs, the methanol gel is reduced in mass. The maximum percentage of depletion should only be 75 wt%, the amount of methanol in the methanol gel.

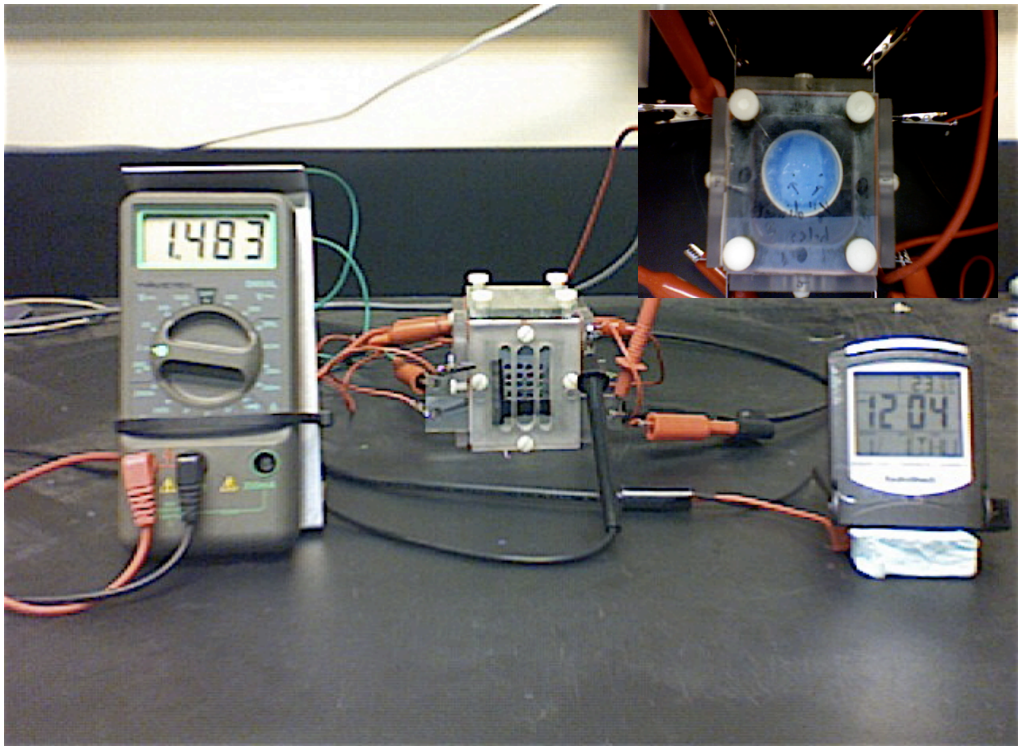

Figure 34: Passive DMFC Powered Clock With Top View

The concept of powering a device was expanded to a small motor propeller connected to an amp meter, which was calibrated with a series resistance of 390 ohms. The fuel cell was connected to the motor to observe voltage and current with respect to time. However, after about 3 hours, the motor broke down (data available in Appendix V). To replicate a motor running, a resistance with an equivalence of 8 ohms was connected to the home-made fuel cell.

Figure 35 represents the current and power trends obtained with respect to time. The fuel cell successfully ran on 20 g of chafing gel for 137 hours before providing zero current. The slight increase in power and current at 5 hours is likely due to the excess air in the methanol reservoir being depleted, allowing a more "pure" environment for the methanol to react. After 5 hours, the power steadily decreases with the voltage. The current doesn't show signs of dropping until after about 20 hours of running. Occasionally, the current and power would start to drop at a steady rate then stabilize for several hours. This is likely due to a chance in the ambient temperature; most of the drops in performance occur at night, when the temperature decreased slightly. Although there is no easy way to observe what is occurring in the methanol compartment, a number of hypotheses can be made. As water and is being formed inside the methanol compartment, the water mostly likely absorbed back into the gel and increased the humidity. This may be a unique feature to resolve the issue of water buildup. As the fuel cell continued to run, carbon dioxide was also produced. However, because there was no direct route for the carbon dioxide to exit from, it either permeated through the MEA or seeped through any possible gaps throughout the fuel cell and was forced out. The carbon dioxide also has a high vapor pressure at room temperature, about 50,000 mm Hg. Compared to the vapor pressure of water and methanol, about 24 mm Hg and 150 mm Hg respectively, it is possible that the high vapor pressure of carbon dioxide is forcing the methanol to the anode sites, improving the reaction rate. From the current-time plot, the capacity was be calculated by equation (8).

$$I = dq/dt \tag{8}$$

Where I is the current, dq is the change in charge, and dt is the change in time. Based on the current recorded from the home-made fuel cell and an integral calculation with the use of Polymath, after 137 total hours of operation, the capacity of the fuel cell was about 8200 mAh. From the power-time plot, the efficiency was calculated by differential equation (9) and equation (10).

$$P = dW/dt \tag{9}$$

$$\varepsilon = W/m{*}\Delta H_{MeOH} \tag{10}$$

Where W is the electric work, m is the mass of methanol, ΔH_{MeOH} is the enthalpy combustion of methanol, and ε is the efficiency of the fuel cell. From the power values recorded from the home-made fuel cell and an integral calculation with the use of Polymath, the work of the fuel cell is about 4600 mWh and the efficiency was calculated at about 5%. Although the efficiency is low, future models of the home-made fuel cell have the potential to provide a notably higher capacity and power.

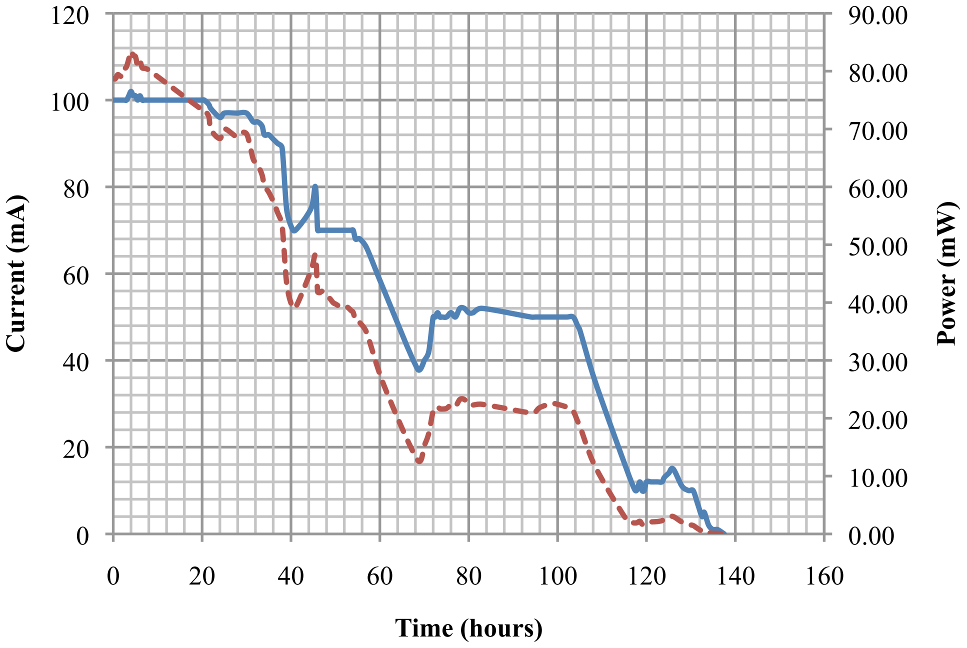

Figure 35: Home-made Fuel Cell Current/Power-Time Plots

Current-time and power-time plots were also obtained from an Energizer AA rechargeable battery (Ni-Mh) as a comparison to the home-made fuel cell (Figure 36). The battery was connected to a 2-ohm resistor and the current was recorded until the battery died. Based on the data acquired from the battery's current-time plot, the capacity was calculated at about 1500 mAh. Although Energizer claims 2450 mAh, the lower calculated capacity was likely due to a low resistance load. In addition, because rechargeable batteries last longer when they are not fully charged, it is possible that the Energizer batteries are restricted to no more than 90% of their full power. Regardless, the battery's capacity is less than a fifth of the home-made fuel cell's capacity, which means the fuel cell can provide a higher amount of current in the same duration of period or the same amount of current for a longer duration of time. The power of the AA battery, derived from the power-time plot, was calculated at about 1250 mWh. While the mass and heat of combustion of the battery are unknown, Michael Fetcenko from ECD

Ovonics claims that Ni-Mh batteries have a specific energy of about 400,000 J/kg (Fetcenko, 2008). Based on the amount of methanol gel consumed in the home-made fuel cell, about 16 g, the specific energy is about 1,030,000 J/kg, just over 2.5 times more than the battery.

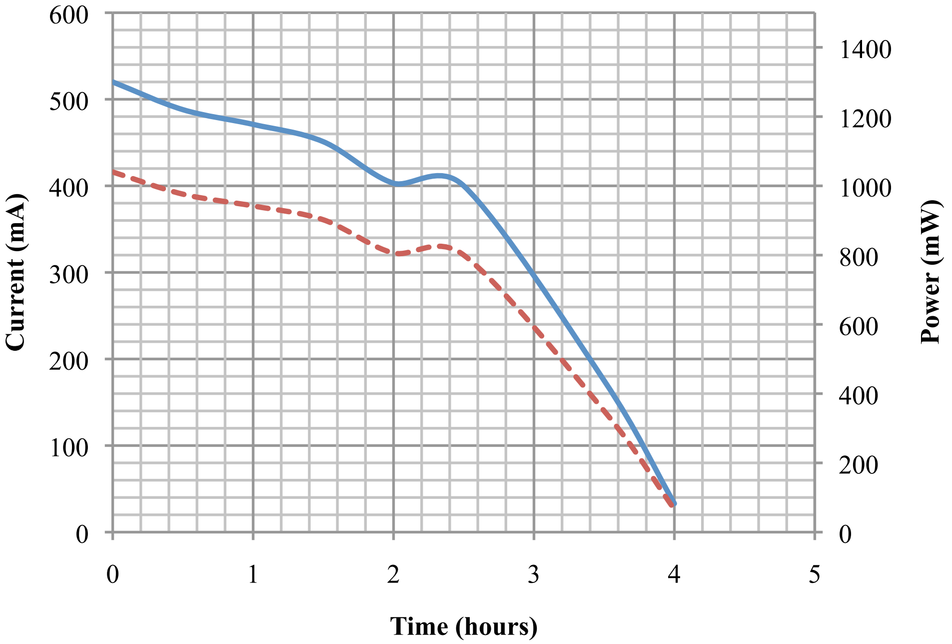

Figure 36: Battery Current/Power-Time Plots

Conclusions & Recommendations

While both “Active” Direct Methanol Fuel Cells and Passive Direct Methanol Fuel Cells have a promising future for providing energy, both have their pros and cons. Active DMFCs are more efficient in providing energy due to access to equipment that allows optimal settings, such as a monitored oxygen flow and a high operating temperature, thereby increasing the reaction rate and improving performance. Passive DMFCs abandon the equipment in exchange for portability, simplicity, and convenience. Despite its performance being hindered to a notable extent, passive DMFCs still show potential for use in portable devices such as audio players and cell phones.

The home-made passive fuel cell I built was originally intended to power a 3rd generation iPod. While the 4-cell fuel cell can meet the current density requirement easily, the voltage requirement cannot be met without several additional MEAs. Therefore, the home-made fuel cell may be more suited for a device with a lower voltage requirement, around 1.5 V.

A variety of options are available as a fuel source in passive DMFCs. Dilute (< 5M) liquid fuel produces a higher voltage at low current densities, which makes accumulating higher voltages easier. However, there is virtually no difference in the current density provided by dilute liquid and pure methanol vapor fuel. An alternative source of fuel to be considered for passive DMFC research is methanol chafing gel. Although the methanol gel vapor fuel does not provide as much power density as pure methanol vapor fuel, it shows potential as a highly convenient fuel source due to its amorphous solid state as well as the omission of preliminary preparation, such as mixing the methanol with water to produce lower concentrations. It is also inexpensive and readily available.

When compared to an Energizer AA rechargeable battery, it outperforms both in how much current and power the home-made fuel can provide. The capacity and specific energy of the home-made fuel cell is about 8,200 mAh and 1,030,000 J/kg, respectively. Compared to the capacity and specific energy of the battery, about 1,500 mAh and 400,000 J/kg respectively, the home-made fuel cell outperforms the battery both in capacity and in energy provided per mass of fuel. If the home-made fuel cell were to be further developed, it has the potential to be several times better than its current model.

Due to time constraints, there were several objectives that were not attained. The research in the home-made passive DMFC has great potential and should be tested further. The following recommendations have been suggested for future research:

- Create a Standard Operations Procedure (SOP) to ensure all equipment and products work properly. Precious time was lost due to the assumption that everything used was working properly.
- Use the original MEA fabrication method as provided by Gleason et al (Gleason et al., 2008). Although the process remains unchanged between that recipe for the home-made catalysts and Field's home-made catalysts (Field, 2008), Gleason had much more success, made apparent by their results.
- Avoid buying the ElectroChem electrodes. Although they have had some success in the past, the most recent studies with these electrodes have shown a very low current density and power output compared to a standard MEA.

- Determine a way to produce a higher temperature naturally, such as a different material of construction for the cell.
- Continue to vary and test different parameters with the home-made passive DMFC, such as membrane thickness.
- Analyze how the methanol gel reacts and what occurs inside the methanol compartment through process modeling.
- Apply other concepts provided in the literature review to enhance performance, such as different current collector composition and the removal of the cathode GDL.
- Determine if a forced flow of air provided by a fan improves performance, and how much it improves performance.
- If feasible, expand the concept of the home-made fuel cell to allow for enough MEAs to power an iPod.

References

Apple. (2009). "*iPod and iPhone Battery and Power Specifications iPod and iPhone Model Range". Online version available at:* http://www.ipodbatteryfaq.com/ipodbatteryandpower.html

Arbizzani, C., Biso, M., Manferrari, E., Mastragostino, M. "Methanol oxidation by pEDOT-pSS/PtRu in DMFC." *Journal of Power Sources*. 178 (2008): 584-590.

Baglio, V., A. Stassi, F. V. Matera, V. Antonucci, and A. S. Arico. "Investigation of passive DMFC mini-stacks at ambient temperature." (2008).

Casalegno, A., Marchesi, R. and Rinaldi, F. "Systematic Experimental Analysis of a Direct Methanol Fuel Cell." *Journal of Fuel Cell Science and Technology*, 4 (2007): 418-424.

Chen R. and Zhao T. S. A novel electrode architecture for passive direct methanol fuel cells [Journal]. - Hong Kong SAR : Electrochemistry Communications, 2007. - Vol. 9.

Chen R. and Zhao T. S. Performance characterization of passive direct methanol fuel cells [Journal]. - Hong Kong : Journal of Power Sources, 2007. - 1 : Vol. 167.

Chen R. and Zhao T. S. Porous current collectors for passive direct methanol fuel cells [Journal]. - Hong Kong : Electrochimica Acta, 2007. - Vol. 52.

Chen, C. Y., & Yang, P. (2003). Performance of an air-breathing direct methanol fuel cell. *Journal of Power Sources, 123*(1), 37-42.

De Renzo, D.J. (1985). Corrosion Resistant Materials Handbook (4th Edition). William Andrew Publishing/Noyes. Online version available at: http://knovel.com/web/portal/browse/display?_EXT_KNOVEL_DISPLAY_bookid=373&VerticalID=0

Eccarius, S., Tian, X., Krause, F., & Agert, C. (2008). Completely passive operation of vapor-fed direct methanol fuel cells for portable applications. *Journal of Micromechanics and Microengineering, 18*(10) Retrieved from http://dx.doi.org/10.1088/0960-1317/18/10/104010

Faghri, A., & Guo, Z. (2008). An innovative passive DMFC technology. *Applied Thermal Engineering, 28*(13), 1614-1622.

Fetcenko, M. (2008, March 19). “Advanced Materials for Next Generation NiMH Batteries”. ECD Ovonic. Retrieved April 27, 2009.

Field, A. “Exploring Operating Conditions and Nafion Membranes for the Direct Methanol Fuel Cell (DMFC).” Major Qualifying Project Report, Worcester Polytechnic Institute, (2008).

Fuel Cell Handbook. 7th ed. (2004) retrieved from: http://www.cleanfuelcellenergy.com/FCHandbook7.pdf

Gleason, D.A., Jensen, K.G., and Painuly, G. “Proton exchange membranes and membrane electrode assemblies for enhanced direct methanol fuel cell performance.” Major Qualifying Project Report, Worcester Polytechnic Institute, (2008).

Hackquard Alexandre Improving and Understanding Direct Methanol Fuel Cell Performance [Report]. - Worcester, MA : Worcester Polytechnic Institute, 2005.

Hoogers, G. “Fuel Cell Technology Handbook.” CRC Press LLC (2003).

Jung, G.B., Su, A., Tu, C.H. and Weng, F.B. “Effect of Operating Parameters on the DMFC Performance.” *Journal of Fuel Cell Science and Technology*, 2 (2005): 81-85.

Kim, D., Cho, E. A., Hong, S., Oh, I., & Ha, H. Y. (2004). Recent progress in passive direct methanol fuel cells at KIST. *Journal of Power Sources, 130*(1-2), 172-177. Retrieved from http://dx.doi.org/10.1016/j.jpowsour.2003.12.023

Kim, H. (2006). Passive direct methanol fuel cells fed with methanol vapor. *Journal of Power Sources, 162*(2), 1232-1235.

Kim, Y., Bae, B., Scibioh, M. A., Cho, E., & Ha, H. Y. (2006). Behavioral pattern of a monopolar passive direct methanol fuel cell stack. *Journal of Power Sources, 157*(1), 253-259. Retrieved from http://dx.doi.org/10.1016/j.jpowsour.2005.06.037

Liu J. G., Zhao T. S., Liang Z. X., Chen R. Effect of membrane thickness on the performance and efficiency of passive direct methanol fuel cells [Journal]. - Hong Kong : Journal of Power Sources, 2005. - 1 : Vol. 153.

Liu Jianguo, Zhao Tian-Shou, Chen Rong, Wong Chung Wai Effect of methanol concentration on passive DMFC performance [Journal]. - Hong Kong SAR : Fuel Cells Bulletin, 2005.

Lu, G.Q. and Wang, C.Y. “Development of High Performance Micro DMFCS and a DMFC Stack.” *Journal of Fuel Cell Science and Technology*, 3 (2006): 131-136.

Oberg, E.; Jones, F.D.; Horton, H.L.; Ryffell, H.H. (2000). Machinery's Handbook (26th Edition). Industrial Press.

O'Hayre Ryan, Cha Suk-Won, Colella Whitney, Prinz Fritz B. Fuel Cell Fundamentals [Book]. - Hoboken, NJ : John Wiley & Sons, Inc., 2006.

Rice, J., & Faghri, A. (2008). Analysis of a passive vapor feed direct methanol fuel cell. *International Journal of Heat and Mass Transfer, 51*(3-4), 948-959. Retrieved from http://dx.doi.org/10.1016/j.ijheatmasstransfer.2007.08.025

Schultz Thorsten, Zhou Su and Sundmacher Kai Current Status of and Recent Developments in the Direct Methanol Fuel Cell [Journal]. - [s.l.] : Chemical Engineering Technology, 2001. - 12 : Vol. 24.

Shimizu, T., Momma, T., Mohamedi, M., Osaka, T., & Sarangapani, S. (2004). Design and fabrication of pumpless small direct methanol fuel cells for portable applications. *Journal of Power Sources, 137*(2), 277-283.

Shukla, Ashok, Martin Hogarth, Paul Christensen, and Andrew Hamnett. "The Design and Construction of High-Performance Direct Methanol Fuel Cells." Power Sources (1997).

Wesley, John N., Amjad Farooq, Ammanuel Mehretaeb, and Francis T. Barbato. Gelled organic liquids. Candle Corporation of America, assignee. Patent 5773706. 1998.

Yang, C., Chiu, S., & Chien, W. (2006). Development of alkaline direct methanol fuel cells based on crosslinked PVA polymer membranes. *Journal of Power Sources, 162*(1), 21-29.

Acknowledgements

I would like to thank the following people for assisting me with this project:

- Professor Datta for giving me the opportunity to expand on his research, allowing me to work on this exciting project, and setting high goals in order to broaden my knowledge in fuel cell research.
- Saurabh Vilekar for providing assistance in many ways, including answering any questions I had, offering input and suggestions, discussing any results obtained and what directions I could go with them, and driving me to various locations when necessary.
- Jack Ferraro and Doug White for help creating the fuel cell from scratch as well as potential materials of construction ideas and input on how to make the device run more efficiently.
- Annemarie Field for working alongside me in the first half of the school year and being a great and enjoyable partner.
- Ashley Millette for showing an interest and passion in fuel cell research.

Appendix I: Treatment Procedure of Home-Made Catalyst Ink

8:30	1 hour	Cut a 2.0 inch X 2.0 inch sheet of Nafion 117 and boil (setting: 3.5) in 300 mL DI water.
9:00	15 min	Prepare anode side catalyst. Zero small beaker on the scale. Add 24 mg PtRu with scalpel Add DI water with dropper. Rinse the sides of the beaker if Pt is stuck to it. 1-2 drops Add 35 mg of 10% Nafion with the dropper. Stir in 5 mL methanol with the scalpel. Cover with parafilm and note on there what it is and when it was prepared. Put in sonicater for **3 hours**. Turn knob to “hold” and turn heat off. Make sure the beaker is sealed well and the parafilm stays above the water. Don’t leave it longer, because ink will evaporate. Keep water cold with ice cubes or refresh every 30-45 min.
9:30	1.5 hours	Low boil in 150 ml 3% H_2O_2
10:40	20 min	Prepare cathode side catalyst (Pt). Put in sonicator for 3 hours.
11:00	1 hour	Low boil in 300 mL DI water.
12:00	10 min	Press membrane if not flat without any heat or pressure
12:10	1h30min	Spray anode side.
1:40	1h30min	Spray cathode side.
3:10	1h30 min	Put membrane in watch glass and cover with Kim wipe. Heat in oven upstairs at 70C
4:50	5 min	Remove membrane from oven with gloves.
4:55	1h30min	Low boil in 200 mL of 0.5M H_2SO_4.
6:30	1h	Low boil in 200 mL DI water
7:30	5 min	If not flat, press for 5 min without heat.
7:35	15 min	Turn on hotpress at 275F. Cut small squares out of the carbon cloth. The square is size of metal bar. (The smooth side of the carbon cloth faces the catalyst). Put the smooth side down and place the metal bar on the rough side. With a scalpel cut around bar. Tape SMOOTH white Teflon paper onto the metal book on both sides. Put carbon cloth rough side down. Then the catalyst on the membrane. Then carbon cloth smooth side down. THE TRICK IS TO ALLIGN EVERYTHING. (2 metric ton for 2 min.)
7:55	10 min	Remove plates from hotpress after 2 min and allow to cool.
8:05		Place hotpressed membrane in fresh zip lock bag and mark with date, type of membrane and treatment.

Appendix II: Preparation of Solutions

<u>1000mL of 3 wt % H_2O_2:</u>
Measure 85.7 mL of 35 wt % H_2O_2
Add 914 mL water

<u>1000 mL of 0.5M H_2SO_4:</u>
Measure 27 mL of 98 wt % $H_2\ SO_4$
Add 973 mL water

<u>Molar concentration of methanol:</u>
1000 mL **1M** methanol → 32.0 g methanol
1500 mL **1M** methanol → 48.1 g methanol

1000 mL **3M** methanol → 96.1 g methanol
1500 mL **3M** methanol → 144.2 g methanol

1000 mL **5M** methanol → 160.2 g methanol
1500 mL **5M** methanol → 240.3 g methanol

1000 mL **7M** methanol → 226.8 g methanol
1500 mL **7M** methanol → 340.2 g methanol

1000 mL **10M** methanol → 320.4 g methanol
1500 mL **10M** methanol → 480.6 g methanol

Appendix III: Calibration of Wavetek Voltage Device

Actual Voltage is the voltage read from the 6060B Electronic Load Box.

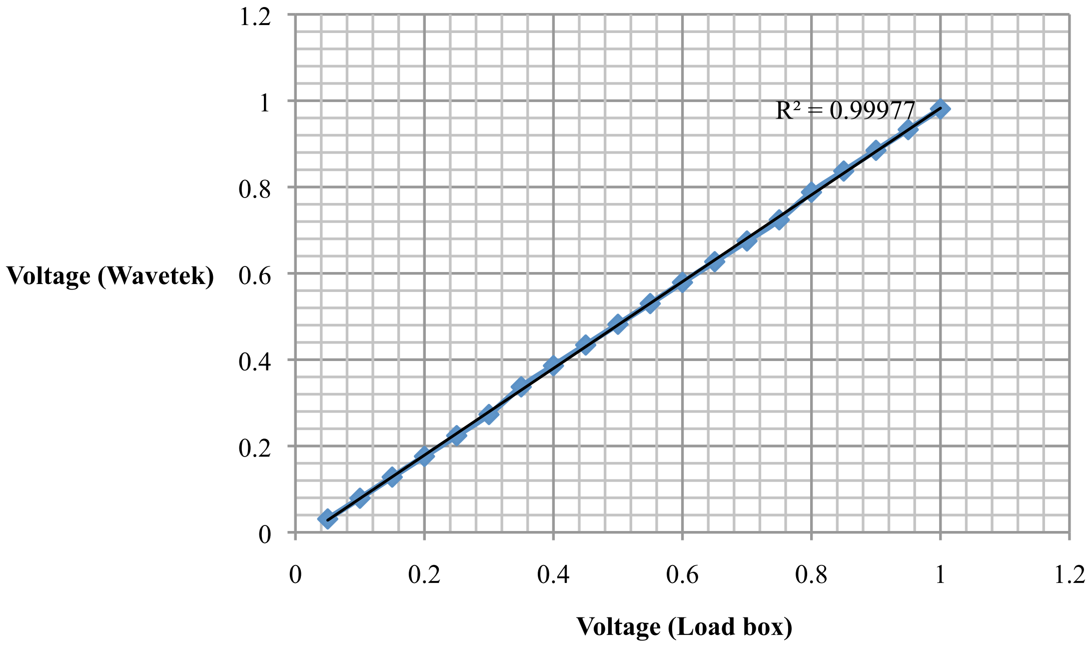

Appendix IV: MSDS for Methanol Chafing Gel

MATERIAL SAFETY DATA SHEET

This form may be used to comply with OSHA's Hazard Communication Standard, 29 CFR 1910.1200. To be valid all information required by 1910.1200(g) of the Standard must appear on this form. Consult the Standard for specific requirements. Note: Blank spaces are not permitted. If any item is not applicable, or no information is available, the space must be marked to indicate that. Quick Name Identifier/Common Name: Chafing Dish Fuel
Methanol Gel UPC/SKU: PH0001, PH0007, PH0020, PH0024, PH0040, PH0080

SECTION 1 – CHEMICAL PRODUCT AND COMPANY IDENTIFICATION

Manufacturer's Name:
Candle Lamp Company
1799 Rustin Avenue
Riverside, CA 92507
For Ben E Keith
24 Hour Emergency Telephone Number:
1-800-255-3924 or 1-813-977-3668 (Collect Calls Accepted)
Information Telephone Number: 1-951-682-9600
Date Prepared: 07/27/07
General or Generic Name: SOLIDIFIED METHANOL / GELLED METHANOL

SECTION 2 – COMPOSITION / INFORMATION ON INGREDIENTS

Ingredients CAS No. % By Weight
Methanol 67-56-1 75.0
Denatonium Benzoate (Bitrex) 3734-33-6 Trace
Mono-Ethylene Glycol 107-21-1 Trace

SECTION 3 – HAZARDS IDENTIFICATION

Potential Health Effects: Methanol (CAS 67-56-1) is the only ingredient expected to have any potential health effects in this product. Methanol is toxic if ingested. Eye/Ocular: Exposure may cause eye irritation. Symptoms may include stinging, tearing, and redness. Skin/Dermal Exposure may cause mild skin irritation. Prolonged, repeated exposure may dry the skin. Symptoms may include redness, burning, drying and cracking, and skin burns. Skin absorption can occur, symptoms may occur similar to inhalation. Swallowing/Ingestion Swallowing is toxic. Usual fatal human dose between 3 oz and 4 oz. Symptoms possible are alcoholic breath, central nervous system depression, convulsions, and coma. Inhalation Exposure to vapor is possible. Short-term inhalation toxicity is low. Breathing small amounts during normal handling is not likely to cause harmful effects; breathing large amounts may be harmful. Symptoms are more likely to be observed at concentrations exceeding recommended exposure limits, and may include headache, drowsiness, nausea, vomiting, blurred vision, blindness, and coma.

SECTION 4 – FIRST AID MEASURES

Eyes: Move individual away from exposure. Flush eyes with plenty of water for at least 15 minutes while holding eyelids open. Seek medical attention immediately. Skin: Remove contaminated clothing. Wash exposed area with warm water for at least 15 minutes. Get medical attention. Wash clothing and shoes before reuse. Swallowing: If swallowed, seek medical attention immediately. If individual is drowsy or unconscious, do not give anything by mouth. If individual is conscious and alert, INDUCE VOMITING. If possible, do not leave person unattended. Inhalation: Move individual away from exposure and into fresh air. If not breathing, give artificial respiration. If breathing is difficult, administer oxygen. Keep person warm and quiet;

seek medical attention immediately.

SECTION 5 – FIRE FIGHTING MEASURES

Flash Point (Method) 54oF (12.2oC) (TAG Closed Cup)
Auto-ignition No data
Explosive Limit Lower Limit: 6.0% Upper Limit 36%
Extinguishing Media CO2, Foam, Dry Chemical (Water may be ineffective)
Fire and Explosion Hazard Vapors form from this product and may travel along the ground/floor or moved by ventilation. Can be ignited by pilot light, flames, sparks, heaters, electric motors or other ignition sources. Do not use heat or flame around closed containers, containers may explode and scatter burning gel. Fire Fighting Instructions Water may be ineffective to extinguish flame. Water may be used to cool fire-exposed containers until fire is extinguished. Wear self-contained breathing apparatus and full protective clothing.
NFPA Rating: 0-Least, 1-Slight, 2-Moderate,
3-High, 4-Extreme Acute Health – 1; Flammability – 3; Reactivity – 0

SECTION 6 – ACCIDENTAL RELEASE MEASURES

Spill: Make sure there is adequate ventilation. Remove all ignition sources. Absorb spill on vermiculite paper. Clean area with water until all material is absorbed and removed.
Large Spill: Immediately eliminate all ignition sources (open flames, smoking materials, pilot lights, electrical sparks). Remove persons not in appropriate protective gear from area. Stop spill at source. Prevent material from entering drains, sewers and waterways. Prevent spill from spreading. Spread absorbent material on spill. Remove to containers for disposal per local, state, and federal ordinances.

SECTION 7 – HANDLING AND STORAGE

Handling Keep away from heat, flame, and sparks. Avoid breathing vapors. Avoid contact with skin, wash thoroughly after handling. Keep away from children. Place can in chafer before lighting, and keep away from combustibles (e.g., paper plates, napkins, paper tablecloths, etc.). Use in a well-ventilated area. DO NOT TAKE INTERNALLY. Storage Containers should be stored away from flame, heat or other ignition sources. Store in a cool dry place (40-120°F, 4-49°C). Provide adequate ventilation. Keep container closed when not in use.

SECTION 8 – EXPOSURE CONTROLS / PERSONAL PROTECTION

Precautionary Labeling WARNING: Keep away from children. Flammable mixture. Do not use near fire or heat. Vapor harmful. May be fatal or cause blindness if swallowed. Cannot be made non-poisonous. Eye Protection Avoid eye contact with material. Skin Protection Avoid contact with skin. Do not remove gel from container. Protective Clothing Recommend the use of rubber or Neoprene gloves and safety goggles. Respiratory Protection Not required unless exposed to high concentrations above approved guidelines.
Exposure Guidelines Methanol 75% OSHA PEL =200 ppm (TWA); ACGIH TLV = 200 ppm (TWA)

SECTION 9 – PHYSICAL DATA AND CHEMICAL PROPERTIES

Appearance and Odor Blue thick gel with alcohol odor
pH ~7 (neutral)
Freeze Range -130 F (-90 C)
Boiling Range 170.6-176 F (77-80 C)
Evaporation Rate 3.5 (Butyl Acetate = 1)
Vapor Pressure 97.68 mmHG @ 68 F (20C)
Vapor Density 1.11 (Air = 1)
Solubility in water Miscible

10. STABILITY AND REACTIVITY

Hazardous Polymerization Will not occur
Hazardous Decomposition Burning may cause carbon dioxide and/or carbon monoxide if inadequate oxygen
Chemical Stability Stable
Incompatibility Heat, open flames and strong oxidizers.

11. TOXICOLOGICAL INFORMATION – NA

12. ECOLOGICAL INFORMATION – NA

13. DISPOSAL INFORMATION

Disposal: Dispose of in accordance with all applicable Federal, State, and local regulations. Purchaser is responsible for proper waste disposal of any partial to full containers. Do not dump into sewers, any bodies of water or onto ground.

14. TRANSPORTATION

Domestic: Consumer Commodity ORM-D
International: Flammable Solid, Organic, n.o.s., (contains methanol), 4.1, UN 1325, PGII

15. REGULATORY INFORMATION

OSHA This product hazardous under the OSHA Hazard Communication Standard (29 CFR 1910.1200)
CERCLA The Reportable Quantity for Methanol is 5000 lbs. Releases equal to or greater must be reported to the National Response Center (NRC) at 800-424-8802.
RCRA The hazardous waste number for Methanol is U154.
SARA 302 Components: None
SARA 313 Components: Methanol (CAS # 67-56-1)
Canada: DSL. The intentional ingredients of this product are listed. International Regulations
EEC: EINECS. The intentional ingredients of this product are listed.
State and Local Regulations
California Proposition 65: None
Pennsylvania: This product is considered unlawful in the state of Pennsylvania (18 P.S. Section 7302(a))
New Jersey Right To Know:: Methyl Alcohol (67-56-1)

16. OTHER INFORMATION

The above data is based on tests and experience, which Candle Lamp Company believes reliable and is supplied for informational purposes only. The Candle Lamp Company's products are intended for sale to industrial and commercial customers. Candle Lamp Company requests that customers inspect and test our products before use and satisfy themselves as to contents and suitability. Some information presented and conclusions drawn herein may be from sources other than direct test data on the substance itself. Candle Lamp Company disclaims any liability for damage or injury which results from the use of the above data, and nothing contained therein shall constitute a guarantee, warranty (including warranty or merchantability) representation (including freedom from patent liability) by the Candle Lamp Company with respect to data, the product described, or their use for any specific purpose, even if that purpose is known to Candle Lamp Company.

Appendix V: Data And Results

CFCE MEA: Clean Fuel Cell Energy Membrane Electrode Assembly
RT: Room Temperature

CFCE MEA, 1M, 70ºC, active			
Voltage (V)	Current (A)	Current Density (mA/cm^2)	Power (mW/cm^2)
0.53	0	0	0
0.5	0.01	2	1
0.4	0.11	22	8.8
0.3	0.39	78	23.4
0.2	0.58	116	23.2

CFCE MEA, 3M, 70ºC, active			
Voltage (V)	Current (A)	Current Density (mA/cm^2)	Power (mW/cm^2)
0.5	0	0	0
0.4	0.1	20	8
0.3	0.46	92	27.6
0.2	0.91	182	36.4

CFCE MEA, 5M, 70ºC, active			
Voltage (V)	Current (A)	Current Density (mA/cm^2)	Power (mW/cm^2)
0.49	0	0	0
0.4	0.05	10	4
0.3	0.25	50	15
0.2	0.6	120	24

CFCE MEA, 7M, 70ºC, active			
Voltage (V)	Current (A)	Current Density (mA/cm^2)	Power (mW/cm^2)
0.47	0	0	0
0.4	0.02	4	1.6
0.3	0.15	30	9
0.2	0.43	86	17.2

CFCE MEA, 50% MeOH, vapor			
Voltage (V)	Current (A)	Current Density (mA/cm^2)	Power (mW/cm^2)
0.27	0	0	0
0.15	0.01	2	0.3
0.1	0.02	4	0.4

CFCE MEA, 100% MeOH, vapor			
Voltage (V)	Current (A)	Current Density (mA/cm^2)	Power (mW/cm^2)
0.32	0	0	0
0.3	0.01	2	0.6
0.25	0.05	10	2.5
0.2	0.08	16	3.2
0.15	0.12	24	3.6
0.1	0.16	32	3.2

CFCE MEA, chafing gel, vapor			
Voltage (V)	Current (A)	Current Density (mA/cm^2)	Power (mW/cm^2)
0.34	0	0	0
0.3	0.02	4	1.2
0.25	0.05	10	2.5
0.2	0.08	16	3.2
0.15	0.11	22	3.3
0.1	0.15	30	3

CFCE MEA, 1M liquid, RT, passive			
Voltage (V)	Current (A)	Current Density (mA/cm^2)	Power (mW/cm^2)
0.47	0	0	0
0.3	0.03	6	1.8
0.2	0.05	10	2
0.1	0.08	16	1.6

CFCE MEA, 3M liquid, RT, passive			
Voltage (V)	Current (A)	Current Density (mA/cm^2)	Power (mW/cm^2)
0.47	0	0	0
0.4	0.01	2	0.8
0.3	0.04	8	2.4
0.2	0.07	14	2.8
0.1	0.13	26	2.6

CFCE MEA, 5M liquid, RT, passive			
Voltage (V)	Current (A)	Current Density (mA/cm^2)	Power (mW/cm^2)
0.46	0	0	0
0.4	0.01	2	0.8
0.3	0.05	10	3
0.2	0.1	20	4
0.1	0.16	32	3.2

CFCE MEA, 7M liquid, RT, passive			
Voltage (V)	Current (A)	Current Density (mA/cm^2)	Power (mW/cm^2)
0.45	0	0	0
0.4	0.01	2	0.8
0.3	0.04	8	2.4
0.2	0.08	16	3.2
0.1	0.15	30	3

Fully assembled cell with 4 CFCE MEAs, chafing gel, RT			
Voltage (V)	Current (A)	Current Density (mA/cm^2)	Power (mW/cm^2)
1.63	0	0	0
1.4	0.01	2	2.8
1.2	0.03	6	7.2
1	0.06	12	12
0.8	0.08	16	12.8
0.6	0.11	22	13.2
0.4	0.15	30	12
0.2	0.18	36	7.2

Motor Data			
Time (hr)	Voltage (V)	Current (mA)	Power (mW)
0	0.92	100	92.00
0.5	0.82	80	65.60
1	0.75	75	56.25
1.5	0.75	75	56.25
2	0.75	75	56.25
2.5	0.73	74	54.02
3.5	1	105	105.00
Inconsistent data; experiment ceased			

3M	1035	liquid	active
Voltage (V)	I (current)	I (current density)	P (power density)
0.2	0.05	10	2
0.3	0.02	4	1.2
0.4	0.01	2	0.8
0.45	0	0	0

3M	1035	vapor	active
Voltage (V)	I (current)	I (current density)	P (power density)
0.2	0.05	10	2
0.3	0.03	6	1.8
0.4	0.01	2	0.8
0.47	0	0	0

3M	115	liquid	active
Voltage (V)	I (current)	I (current density)	P (power density)
0.2	0.16	32	6.4
0.3	0.03	6	1.8
0.4	0.01	2	0.8
0.49	0	0	0

3M	115	vapor	active
Voltage (V)	I (current)	I (current density)	P (power density)
0.2	0.16	32	6.4
0.3	0.06	12	3.6
0.4	0.01	2	0.8
0.41	0	0	0

5M	1035	liquid	active
Voltage (V)	I (current)	I (current density)	P (power density)
0.2	0.07	14	2.8
0.3	0.03	6	1.8
0.4	0.01	2	0.8
0.49	0	0	0

5M	1035	vapor	active
Voltage (V)	I (current)	I (current density)	P (power density)
0.2	0.03	6	1.2
0.3	0.01	2	0.6
0.4	0.01	2	0.8
0.49	0	0	0

5M	115	liquid	active
Voltage (V)	I (current)	I (current density)	P (power density)
0.2	0.11	22	4.4
0.3	0.05	10	3
0.4	0.01	2	0.8
0.49	0	0	0

5M	115	vapor	active
Voltage (V)	I (current)	I (current density)	P (power density)
0.2	0.05	10	2
0.3	0.02	4	1.2
0.4	0.01	2	0.8
0.52	0	0	0

Toy Car MEA, active, 70ºC, 1M			
Voltage (V)	Current Density (A)	Current Density (mA/cm^2)	Power Density (mW/cm^2)
0.2	0.38	76	15.2
0.3	0.17	34	10.2
0.4	0.05	10	4
0.52	0	0	0

Toy Car MEA, active, 70ºC, 3M			
Voltage (V)	Current Density (A)	Current Density (mA/cm^2)	Power Density (mW/cm^2)
0.2	0.38	76	15.2
0.3	0.15	30	9
0.39	0	0	0

Toy Car MEA, active, 70ºC, 5M			
Voltage (V)	Current Density (A)	Current Density (mA/cm^2)	Power Density (mW/cm^2)
0.2	0.31	62	12.4
0.3	0.11	22	6.6
0.4	0	0	0

Fully Assembled Cell, Time Depent Graphs			
Time (hr)	Voltage (V)	Current (mA)	Power (mW)
0	0.787	98.375	77.42
0.5	0.787	98.375	77.42
1	0.794	99.25	78.80
1.5	0.792	99	78.41
2	0.791	98.875	78.21
2.5	0.803	100.375	80.60
3	0.808	101	81.61
3.5	0.813	101.625	82.62
4	0.818	102.25	83.64
4.5	0.819	102.375	83.85
5	0.817	102.125	83.44
5.5	0.809	101.125	81.81
6	0.809	101.125	81.81
6.5	0.806	100.75	81.20
7	0.805	100.625	81.00
7.5	0.804	100.5	80.80
8	0.802	100.25	80.40
19.5	0.736	92	67.71
20	0.736	92	67.71
20.5	0.732	91.5	66.98

21.5	0.729	91.125	66.43
22	0.713	89.125	63.55
24	0.712	89	63.37
25	0.722	90.25	65.16
27.5	0.709	88.625	62.84
28	0.712	89	63.37
30	0.713	89.125	63.55
31.5	0.682	85.25	58.14
32.5	0.672	84	56.45
33.5	0.66	82.5	54.45
34	0.655	81.875	53.63
35	0.642	80.25	51.52
36	0.632	79	49.93
37	0.617	77.125	47.59
38	0.599	74.875	44.85
39	0.58	72.5	42.05
40	0.562	70.25	39.48
41	0.559	69.875	39.06
44.5	0.607	75.875	46.06
45.5	0.602	75.25	45.30
46	0.598	74.75	44.70
46.5	0.596	74.5	44.40
47	0.599	74.875	44.85
48.5	0.584	73	42.63
49	0.578	72.25	41.76
49.5	0.571	71.375	40.76
50	0.568	71	40.33
51	0.562	70.25	39.48
52	0.562	70.25	39.48
52.5	0.562	70.25	39.48
53.5	0.552	69	38.09
54	0.547	68.375	37.40
54.5	0.543	67.875	36.86
55	0.541	67.625	36.59
55.5	0.537	67.125	36.05
57	0.528	66	34.85
61	0.456	57	25.99
68.5	0.336	42	14.11
70	0.382	47.75	18.24
71	0.414	51.75	21.42
72	0.426	53.25	22.68
72.5	0.436	54.5	23.76
73	0.431	53.875	23.22
73.5	0.433	54.125	23.44
74	0.432	54	23.33
75	0.434	54.25	23.54
76	0.437	54.625	23.87

77	0.441	55.125	24.31
78	0.447	55.875	24.98
79	0.447	55.875	24.98
80	0.439	54.875	24.09
81	0.437	54.625	23.87
83	0.431	53.875	23.22
94	0.418	52.25	21.84
95	0.422	52.75	22.26
96	0.437	54.625	23.87
98.5	0.451	56.375	25.43
99	0.452	56.5	25.54
102	0.439	54.875	24.09
103.5	0.424	53	22.47
104.5	0.406	50.75	20.60
105	0.397	49.625	19.70
108.5	0.331	41.375	13.70
115.5	0.167	20.875	3.49
117.5	0.19	23.75	4.51
118.5	0.183	22.875	4.19
119	0.17	21.25	3.61
119.5	0.167	20.875	3.49
120	0.168	21	3.53
121	0.173	21.625	3.74
121.5	0.175	21.875	3.83
122.5	0.179	22.375	4.01
123.5	0.192	24	4.61
124	0.198	24.75	4.90
125	0.201	25.125	5.05
126	0.201	25.125	5.05
128	0.186	23.25	4.32
129.5	0.161	20.125	3.24
130.5	0.146	18.25	2.66
131.5	0.135	16.875	2.28
132.5	0.128	16	2.05
133	0.125	15.625	1.95
134	0.116	14.5	1.68
135	0.108	13.5	1.46
136	0.106	13.25	1.40
137.5	0.086	10.75	0.92

Time Dependent Graphs (battery)			
Time (min)	Voltage (V)	Current (mA)	Power (mW)
0	1.04	520	1040
0.5	0.976	488	976
1	0.942	471	942
1.5	0.902	451	902
2	0.806	403	806

2.5	0.8	400	800
3.5	0.35	175	350
4	0.066	33	66

Capacity (mAh)	Work (mWh)	Energy Density (J/kg)	Efficiency
8200	4600	1028571	0.0460
mass of gel (g)	mass after fuel cell run (g)	MW of MeOH (g/mol)	moles of MeOH (mol)
20	3.9	32	0.503
ΔH, comb. (kJ/mol)	Q (J)	Q (mWh)	
715	359734	99926	

Ashley Millette's data:

		Open Circuit Potential (Volts)					
		Fan Settings					
		Off		Low		High	
Trial #	**Molarity**	10 min.	20 min.	10 min.	20 min.	10 min.	20 min.
1	1	0.420	0.388	0.375	0.368	0.361	0.353
2	1	0.329	0.321	-	-	-	-
3	3	0.401	0.387	0.380	0.376	0.369	0.361
4	3	0.352	0.342	-	-	-	
5	5	0.330	0.287	0.308	0.290	0.290	0.278
6	5	0.301	0.294	-	-	-	-
7	7	0.435	0.401	0.377	0.372	0.363	0.399
8	7	0.347	0.336	-	-	-	-

	Open Circuit Potential (Volts)	
Membrane #	10 min.	20 min.
115	0.457	0.445
1035	0.448	0.433
117	0.573	0.550
1110	0.609	0.608

		OCP (Volts)	
Trial #	**Molarity**	30 min.	2 hr.
1	3	1.61	1.43
2	Pure	1.01	0.97